2014

BEYOND ROOTS ALONE: NOVEL METHODOLOGIES FOR ANALYZING COMPLEX SOIL AND MINIRHIZOTRON IMAGERY USING IMAGE PROCESSING AND GIS TOOLS

Justina A. Silva
Michigan Technological University

BEYOND ROOTS ALONE: NOVEL METHODOLOGIES FOR ANALYZING COMPLEX SOIL AND MINIRHIZOTRON IMAGERY USING IMAGE PROCESSING AND GIS TOOLS

By

Justina A. Silva

A THESIS

Submitted in partial fulfillment of the requirements for the degree of

MASTER OF SCIENCE

In Applied Ecology

MICHIGAN TECHNOLOGICAL UNIVERSITY

2014

This thesis has been approved in partial fulfillment of the requirements for the Degree of MASTER OF SCIENCE in Applied Ecology.

School of Forest Resources and Environmental Science

Thesis Co-Advisor:	*Dr. Ann Maclean*
Thesis Co-Advisor:	*Dr. Erik Lilleskov*
Committee Member:	*Dr. Amy Marcarelli*
School Dean:	*Dr. Terry Sharik*

TABLE OF CONTENTS

Preface

The main body of this thesis is expected to be submitted to a peer-reviewed journal articles for publication. All work and analysis was conducted by Justina Silva who will serve as primary author. Dr. Ann Maclean and Dr. Erik Lilleskov contributed to experimental design as well as revisions and suggestions on the final manuscript.

Acknowledgements

I am immensely grateful to my advisors Dr. Ann Maclean and Dr. Erik Lilleskov for their guidance, knowledge, and encouragement of creativity. Without their support my education and research would not be possible. I am highly appreciative to everyone at the USFS Northern Research Station for the help with my projects and invaluable input in my writing. I am very thankful for Dr. Amy Marcarelli's willingness to serve on my committee. I cannot thank my officemates in the GIS & Remote Sensing lab enough for the time spent problem solving, in thought provoking conversations, and most importantly companionship. I look forward to future interactions as we grow as land managers and researchers. I am endlessly thankful to my friends and family for their love and support. Lastly, I would like to acknowledge Cameron Anderson, without you my journey would have not lead me to Michigan's UP and to the endless opportunities at Michigan Tech.

Abstract

Quantifying belowground dynamics is critical to our understanding of plant and ecosystem function and belowground carbon cycling, yet currently available tools for complex belowground image analyses are insufficient. We introduce novel techniques combining digital image processing tools and geographic information systems (GIS) analysis to permit semi-automated analysis of complex root and soil dynamics. We illustrate methodologies with imagery from microcosms, minirhizotrons, and a rhizotron, in upland and peatland soils. We provide guidelines for correct image capture, a method that automatically stitches together numerous minirhizotron images into one seamless image, and image analysis using image segmentation and classification in SPRING or change analysis in ArcMap. These methods facilitate spatial and temporal root and soil interaction studies, providing a framework to expand a more comprehensive understanding of belowground dynamics.

Chapter 1: Beyond roots alone: novel methodologies for analyzing complex soil and minirhizotron imagery using image processing and GIS tools[1,2]

1.1 Introduction

1.1.1 The opportunity

Belowground image analysis has most commonly focused on quantifying root dynamics (Chapin & Ruess, 2001, Farrar & Jones, 2000, Jackson *et al.,* 1997, Johnson *et al.,* 2006, Trumbore *et al.,* 2006). However, comprehensive monitoring of visible manifestations of physical, chemical, and biotic dynamics belowground is essential to advance understanding of otherwise hidden soil processes that regulate nutrient cycling, greenhouse gas flux, and soil carbon (C) sequestration. Important visible belowground physical processes include soil wetting fronts, frost heaving, and changes in pore space. Visible chemical changes include redox-dependent reactions, e.g., gleying/mottling of soils; oxidation of organic matter by decomposers; and the formation of methane as manifested in gas bubbles in anoxic wetland soils. Common visible biotic dynamics include root and fungal demographics, root herbivory and fungivory, macroinvertebrate distribution and phenology, and soil macrofauna. Including these factors in belowground monitoring would contribute to a holistic approach that is imperative to advance understanding in the face of challenging fundamental and applied problems.

---

[1] This research will be submitted to a peer-reviewed journal for publication.

[2] All images and software screenshots were created using ArcGIS® software by Esri. ArcGIS® and ArcMap™ are the intellectual property of Esri and are used herein under license. Copyright © Esri. All rights reserved. For more information about Esri® software, please visit www.esri.com.

We do not mean to downplay the importance of roots, which have directly measurable multi-scale importance, from individual physiological processes, through ecosystem level nutrient dynamics and soil organic matter accumulation, to global scale C cycling. Short-lived fine roots represent a substantial input of organic matter and nutrients into the soil (Rasse *et al.,* 2005). Mycorrhizal fungi are a significant mediator between root and soil nutrient uptake and have a substantial impact on carbon sequestration (Veregsoglou *et al.,* 2012). Soil organic matter stores three times more C than the atmosphere or terrestrial vegetation (Schmidt *et al*., 2011). Given anthropogenic changes in global C cycling and their impact on global climate, it is imperative to understand this complex system (Wan et al., 2004). Yet the indirect effects of changing climate and CO_2 on belowground carbon allocation are poorly understood. A better understanding of root dynamics and their effects on soil biogeochemistry is vital, and non-destructive root and soil imagery analysis is requisite for advancing understanding.

Methods for quantifying root growth spatially and temporally using non-destructive methods rely heavily on minirhizotrons, transparent tubes placed permanently in the ground for imaging the rhizosphere (Iversen *et al.,* 2012, Taylor *et al.,* 2014). There are numerous methods for processing minirhizotron imagery, whose strengths and weaknesses are discussed elsewhere (Milchunas, 2009, French *et al.,* 2009, Iversen *et al.,* 2012, Rewald & Ephrath, 2012, Vamerali *et al.,* 2012). Despite the plethora of minirhizotron image analysis techniques, long processing time creates a bottleneck that limits advancement in root demographic studies. To study root demography, images are captured at frequent intervals (Rewald & Ephrath, 2012), often leading to massive

backlogs of unprocessed data. Furthermore, these images encompass a very small area and provide limited information on root system integration.

Beyond minirhizotron techniques, methods for analyzing larger complex root imagery are rudimentary. We have not found an automated method that accurately and efficiently determines root lengths and areas in large complex images with dense root systems grown in natural media. As for minirhizotron image analysis, existing image analysis approaches (Majdi, 1996, Vamerali *et al.,* 2012,) can be quite time consuming and require substantial input from the analyst.

The importance of standardization in using images to perform root and soil observational studies has yet to be addressed in the root studies literature. Resisting the need to enhance imagery is discussed in Rossner & Yamada (2004) in terms of cellular biology; however the same principles need to be considered in belowground image processing. Arbitrarily enhancing an image can produce false turn-over rates as a tan root could appear white under the incorrect lighting. In particular, the issue of color consistency is a considerable challenge when conducting experiments of this kind.

There is a critical need for improved knowledge on fine root structure, quantities, and demography, on as many plant species as possible, for better management and predictions on biogeochemical processes (Pierret *et al.,* 2005, Smithwick *et al.,* 2014). Belowground images contain a wealth of valuable information beyond just roots. Many of the physical, chemical, and abiotic processes occurring belowground are amenable to image analysis (Downie *et al.,* 2014). To our knowledge no other methods have the advantage of simultaneously tracing roots while additionally quantifying other phenomena of interest. We see this as a missed opportunity when such a large wealth of belowground data is

being collected in every image. These analysis procedures fill a need for consistent and accurate tracing capabilities and flexible data management via attribute tables in ArcMap.

1.1.2 *New approaches*

To address these limitations in belowground image analysis, we need easily implemented tools for visual analyses of complex root system dynamics and other soil processes. We propose applying methodologies widely employed and accepted in the fields of remote sensing and photogrammetry. The issues faced while studying belowground imagery are remarkably similar to those encountered with aboveground remotely sensed data, including: large data sets, finding areas of discrete features such as lakes and streams or lengths and widths of roads, change detection and rates of change, and transformation of the imagery to improve interpretability. Here we introduce an innovative application of GIS and remote sensing techniques for the study of roots and soil processes, starting with guidelines for image acquisition, followed by the use of software traditionally used at the landscape level: SPRING (http://www.dpi.inpe.br/spring/) and ArcMap (ESRI, Redlands, CA) for image analyses. Methodologies include image segmentation and classification, change analysis, and the use of basic ArcMap tools and functions. These approaches allow rapid classification and change analysis on large, complex belowground images.

SPRING classifies the entire image utilizing image segmentation, which creates demarcated regions based on pixel proximity and likeness, with thresholds defining user-generated classes. SPRING's interface is user-friendly and requires no knowledge of computing syntax or direct use of complex algorithms. This approach differs from root-centric segmentation algorithms such as Zeng *et al.* (2008, 2010), or Shojaedini &

Heidari (2013), which exclusively identify roots, ignoring rhizosphere processes. These methods also differ from a root-centric GIS-based approach proposed by Gasch *et al.* (2011), who use Feature Analyst to trace roots.

To demonstrate its utility, in the following sections we present SPRING image segmentation and classification on three types of imagery with varying complexities. We also present a method utilizing ArcMap to perform change analysis using image subtraction. This method is commonly used with remotely sensed imagery (Singh, 1989), and performing this type of analysis in ArcMap is much simpler than methods requiring computing syntax. We performed image subtraction followed by thresholding to isolate the values that indicate change on sets of images that represent various soil-root conditions.

In addition to seeking new methods to improve root and soil image processing, we created a novel approach for analysis of minirhizotron images. We mosaicked separate minirhizotron image segments into one continuous image to gain more information per minirhizotron tube. The single larger image allows quantitative image processing techniques to be utilized under conditions of soil and root movement, such as in peatland ecosystems (Iversen *et al.,* 2012) or after frost heaving, which hinder the use of other image analysis software packages. Our novel methods for minirhizotron image analysis include image segmentation and classification for quantifying the standing crop of roots, change detection analysis to derive root production or turnover, and traditional manual tracing techniques using ArcMap in place of conventional root tracing programs. All involve the creation of individual root segments feature layers, which can be analyzed in the supporting attribute table. The creation of root segment layers in ArcMap enables us

to superimpose multiple images of root segments from multiple sample dates over one another. In the following sections we detail these novel approaches.

1.2 **Image Acquisition**

1.2.1 *Image acquisition guidelines*

To view a digital image is to create a brightness map, i.e., a computer graphic display of brightness values (BV) based on reflectance from the feature of interest. Root color change (a change in BV) is the basis for determining root demography and tracing root perimeters. It is common practice to enhance root images to increase the contrast between the background and the features of interest, which is acceptable when manually interpreting a single image. However, when multiple images are being analyzed using semi-automated procedures, standardization of BV between images is essential to obtain correct measurements (Plataniotis *et al.,* 2000). This means camera settings, imaging distance and lighting conditions, and image enhancements must be consistent for all image acquisitions. It is also important to ensure that bright objects are not overexposed when photographed, because overexposure essentially chops off the upper end of the BV range. In minirhizotrons, fully blocking incoming sunlight is essential to maintain constant BVs, as it contributes inconsistent light to the top frames in a minirhizotron tube.

Figure 1.1 illustrates the importance of standardized image acquisition parameters with mosaicked minirhizotron images, each consisting of four frames. Each frame was acquired with different camera settings, resulting in inconsistent BV for roots and peat from frame to frame. Figure 1b displays the same minirhizotron area as Figure 1.1a after 3 months. Within the second frame in both images, the peat is darker in Figure 1.1a than in 1.1b, raising questions regarding the "true" color of the roots. In addition to interfering with quantitative color comparisons over time and space, the image-to-image inconsistency also prevents the image mosaic from appearing seamless.

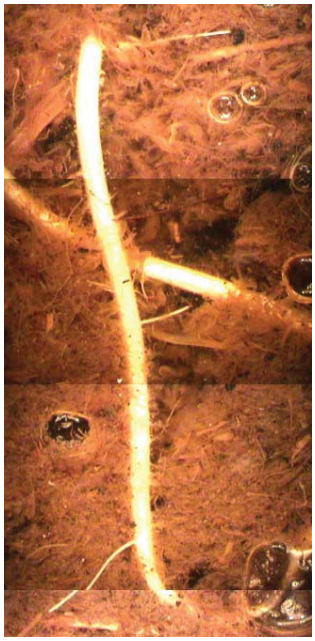

Fig. 1.1a

Fig. 1.1b

Figure 1.1 Two sets of minirhizotron images, acquired at different times that have been mosaicked together demonstrating the importance of camera setting consistency. (a) Image acquired June 2011 with different settings for three frames, (b) Image acquired September 2011 again with different settings between frames.

Inconsistent enhancements that change the apparent color of roots can cause underestimation of maturation or turnover rates. Figure 1.2a, a color-standardized image, shows a dark brown root, indicated by the green arrow. However, Figure 1.2b shows the same root now lighter in color due to image enhancement. This image is over-exposed, and the BV enhanced to make the fine roots stand out (blue arrow) at the expense of overall image color. The fine roots in Figure 1. 2b are more apparent than the fine roots in Figure 1.2a (blue arrows), but this enhancement is unacceptable for quantitative color change measurements.

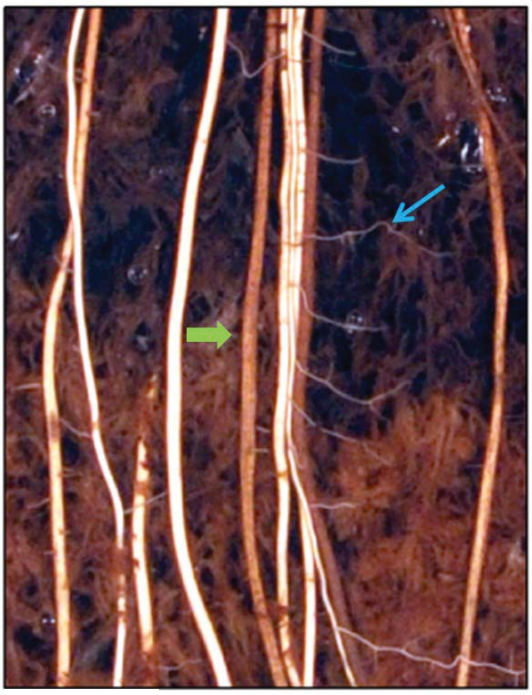

Fig. 1.2a

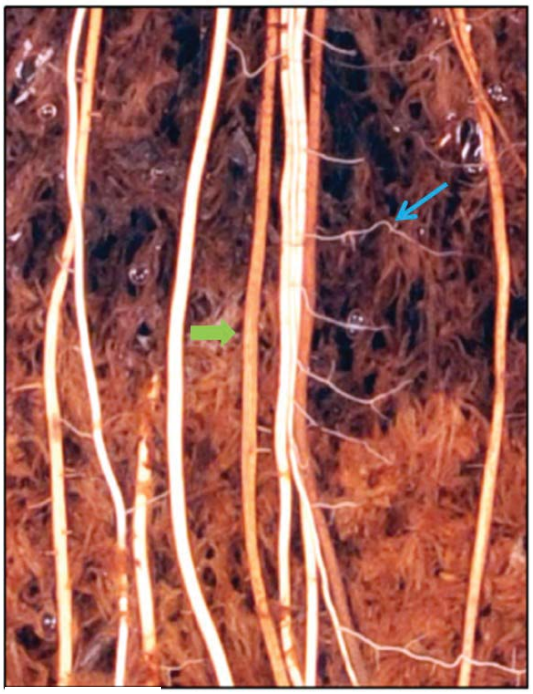

Fig. 1.2b

Figure 1.2 Consecutively acquired images: (a) has been color corrected with a Macbeth ColorChecker (b) had brightness and contrast adjusted to make fine roots more visible.

If standardized camera settings and lighting conditions are not possible, color correction via use of a standard color scale, e.g., Macbeth ColorChecker card (X-rite photo Part# MSCCC), should be considered. The card is a checkerboard array of 24 colored squares in a wide range of colors, providing the needed baseline for comparing, measuring and analyzing objects when true color is required. In cases where enhancing contrast is necessary to make roots or objects more apparent, it is good practice to take two images, one for quantitative color analysis and one for growth measurements.

External lighting is an important consideration in imaging soil systems, as various bulbs emit different wavelengths of light which ultimately affect the color temperature of an image. Fluorescent bulbs produce the whitest light, but may not be appropriate in some systems. Having consistent illumination across an imaged surface is also important, especially when using segmentation algorithms, as it changes BV (Gijsenij *et al.,* 2012). Using an external camera flash attached to the camera can provide more consistent lighting compared to lamps, because of control over shutter speed and aperture (Persichetti *et al.,* 2007). Regardless of the bulb type, it is important to maintain lighting brightness, temperature, and intensity for color consistency.

Additionally, camera type may affect image color. It is impractical to suggest all imagery be acquired using an imaging spectrometer which records light intensities at varying wavelengths, as opposed to commercially available SLR or CCD digital cameras that record visible and near-IR reflectance. However, it is important to recognize that the bandwidths (spectral resolution) labeled blue, green, red and near-IR will vary between camera brands and models. Hence it is recommended the same camera, lens, and filter be used for image acquisition during the life of a project.

1.2.2 *Image acquisition guidelines in use*

To demonstrate these guidelines, we used images from three different types of experimental systems: experimental microcosms, wetland minirhizotrons, and an upland rhizotron facility. The microcosms are small plexiglass containers filled with peat and wetland plants. The microcosms are used to represent a diversity of complex densely-rooted systems. A Nikon D90 camera was used with fixed settings of f-stop/6.3, exposure time 1/160 second, flash off, and an ISO of 640. We used a Nikon micro lens with a 90 mm focal length and a spatial resolution of 0.125 mm. The camera was mounted to a stationary fixture to maintain image capture distance and minimize blur. Blur produces false areas with large-scale imagery especially when using semi-automated image segmentation procedures. A stage was built to hold the root windows and the camera stand was attached. For lighting, we used frosted photoflood bulbs (SYLVANIA 11560) mounted on light stands situated to eliminate glare and produce even illumination. To ensure color consistency we also used a MacBeth ColorChecker. After capture and color correction, these images were registered to a planar X, Y coordinate system (see supplementary protocol for instructions).

Minirhizotron images came from the USDA-Forest Service Houghton Mesocosm Facility, where 24 1-m^3 bins containing peatland plant communities are instrumented to investigate carbon dynamics in a changing climate (Potvin *et. al.*, 2014); within each bin is a minirhizotron tube in which images were collected monthly using a Bartz BTC-100x minirhizotron video microscope (Bartz Technology Corp, Carpinteria, CA). Prior to analysis, imagery from each tube was mosaicked together with a provided ArcMap Tool. The tool automatically stitches images together into a single seamless image, allowing for

analysis of the entire minirhizotron tube rather than individual small regions. This allows analysis of entire root segments that span numerous frames, a significant advantage over traditional methods. Having the minirhizotron images stitched together also allows faster processing times using image segmentation and image subtraction.

Rhizotron images came from the USDA-Forest Service Houghton Rhizotron Facility, which consists of 24 1.5 x 1 m windows providing access to two different forest and soil types. Two types of imagery come from the Rhizotron, automated time lapse photographs and manual photographs. The automated photographs are taken every 30 minutes using a Nikon D50 with a 60 mm f/2.8 D AF Micro-Nikkor fixed lens with an infrared (IR) light source (www.surveillance-spy-cameras.com, Part# SSC IR104 940W). In order to take images with an IR light source our camera was modified (www.maxmax.com) by removing the IR filter, extending the recorded wavelengths from the UV range through the IR range (330nm-1200nm), as opposed to standard cameras recording wavelengths between 400nm-780nm. Lighting, camera settings, and positioning remained consistent between image capture sessions.

Manually captured photos were taken using a custom-made metal imaging box with a stationary synchronized Nikon flash at each side, directly facing each other for complete, glare free, and consistent illumination. The camera used is a Nikon D50 with a 60 mm f/2.8 D AF Micro-Nikkor fixed lens. The distance from glass to lens is fixed. However, the imaging box is moved between the window panes, so the images taken in different sessions do not line up perfectly and had to be georeferenced to one another. Georeferencing is the process of aligning images via an affine transformation to ensure they occupy the same spatial location. This is accomplished by using a minimum of three

control points, which are visible features located in the same place on all the images. The resulting geospatially referenced images can be overlaid and compared quantitatively and qualitatively. ArcMap's online resource center (resources.arcgis.com) provides details on georeferencing. All but one set of images for the study was georeferenced using this process.

1.3 **Image Analysis Methodologies**

Method of analysis depends on the question and image content. The best analysis methodology must be determined by the analyst, emphasizing the art and science that is image processing. Gaining familiarity with these methods and their final products is key in optimizing the functionality of these tools.

1.3.1 *Attribute table*

ArcMap maintains data associated with features in the attribute table. By accessing the information in the attribute table each soil feature is associated with its own attribute ID. Additional data can be entered pertaining to a particular polygon; for example, directly measured variables such as root diameter, color values, species, branching order, or soil depth can be added. The Field Calculator within the attribute table allows the entrance of equations for scaling or correction factors, and the Calculate Geometry function permits automated length and area calculations. Keeping track of objects from prior imaging sessions is done by copying the first session features to the next and re-naming. Soil features positions can be changed when needed; this maintains the attribute table data and retains feature's unique identities. Furthermore the use of the attribute table enables data queries for comparison of root variables over time for better predictions and deeper

understanding of these complex networks. All of the following methodologies for measuring soil features involve the use of the attribute table.

1.3.2 *SPRING Segmentation and classification*

SPRING is an open source image processing software package which uses image segmentation as a classification procedure (Camara *et al.,* 1996, Bins *et al.,* 1996). Image segmentation is a region-growing approach using an algorithm that defines regions within the image based on pixels (seeds) initially defined as unique regions. From these seed pixels, regions are grown by merging neighboring pixels with similar properties (similarity) based on the pixel BVs. The algorithm employs a user-defined similarity parameter that defines region boundaries. The smaller the similarity value chosen, the more similar the BVs of neighboring pixels have to be to be considered the same region. A different region is created when the similarity value is exceeded. Once regions are established they are combined with adjacent regions based on the BV value similarities and minimum region size perimeter as specified by the user.

Once classifying an image there are a number of considerations. When defining classification regions, it is imperative to select well-distributed regions over the entire image. The number of classes needed depends on the color variation of the image and the goals of the classification. An image with uniform soil color will have a class for soil and several classes for roots depending on the BV variation. Finding the best similarity and minimal region size combination for an image (or set of images) is an iterative process and requires analyst involvement. The differences between soil and root (or other matrix and object) color in any given image is the basis for determining similarity value. If the roots and soil have similar colors, starting with a smaller similarity value will potentially

provide the best results. If the soil and roots have good color contrast, a larger similarity value is more appropriate. As new phenomena appear in a set of images the similarity and minimal region size parameters may need to be adjusted.

Optimizing minimal pixel region size is also critical for discrimination between roots and soil. During classification, if minimal pixel region size is too small, soil pixels with coloring similar to root pixels will be misclassified as roots. Table 1 displays the optimal similarity value and minimum region size for each image analyzed with SPRING. In Figure 1.3 there is a portion of a complex root image displaying the steps taken in SPRING to segment and classify an image. Figure 1.3a is the original image; there are slight variations in the BVs of each individual root that could cause roots to be broken into multiple classes. To overcome this problem, a larger minimal pixel region value will force these spectrally varying regions to stay together (Fig. 1.3b), thus minimizing the possibility of an incorrect classification. To initially check the segmentation and classification results, examine the smallest roots in the image; they should be accurately outlined, meaning areas of adjacent soil are separated from segments of root as in Fig. 1.3b. In Fig. 1.3c the fine roots are clearly classified in a fine root region versus a soil region. If root pixels are mistakenly grouped within a soil region, the similarity value should be lowered or the minimal pixel region size value decreased.

Table 1.1 The optimal similarity values and minimal region pixel size used in SPRING for the segmentation of rhizotron, minirhizotron, and microcosm imagery.

Image Type	Similarity Value	Minimal region size
Rhizotron	16	100
Minirhizotron	10	100
Microcosm	5	20

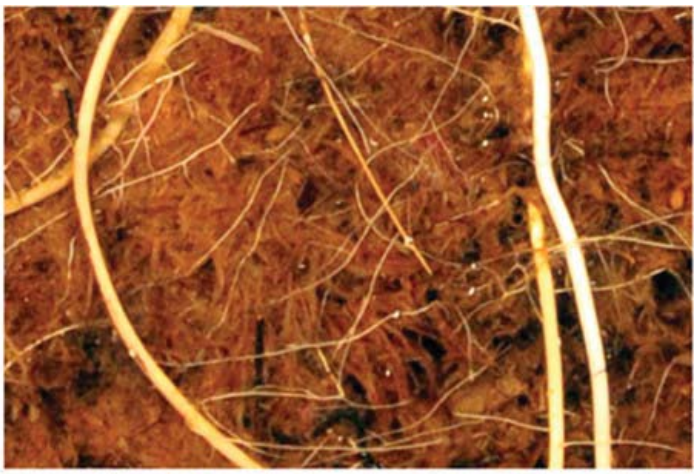

Fig. 1.3a

Fig. 1.3b

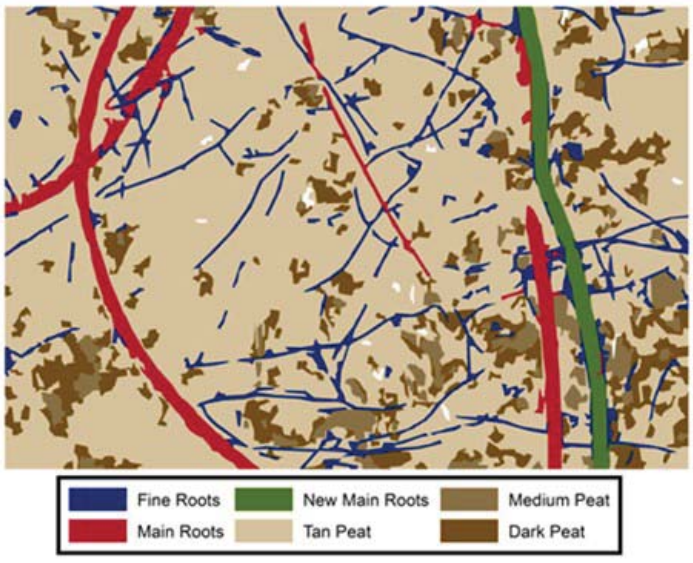

Fig. 1.3c

Figure 1.3 Segmentation and classification of a microcosm image in SPRING: (a) image imported into SPRING, (b) same image segmented into pixel regions for classification, (c) resulting classified image from pixel regions divided into 6 classes.

Once the classification is satisfactory, the single band image can be imported into ArcMap for further spatial analysis. The classified image is turned into vector data, in the form of polygons, and assigned a classification group. Using the Vectorization tool called Generate Features, centerlines are drawn through each root and average diameter is calculated. Areas of soil coloration are also measured here.

1.3.3 SPRING method in use

As a test of the versatility of SPRING segmentation and classification we classified different images, starting with the more complex microcosm images (Fig. 1.4). These images have a large variety of soil color; in some instances the color of the peat soil matched the color of fine roots. Figure 4a also had areas of blackening around roots that are of interest, as they likely indicate root-mediated oxidation of the rhizosphere in an otherwise anaerobic soil environment, and so they received a separate class as well (Fig. 1.4b). The resulting classification (Fig. 1.4b) has two peat classes, dark brown peat and light brown peat (transparent in figure); two root classes, main roots (fuchsia) and fine roots (cyan); and one class for blackened peat (navy). The best segmentation threshold for the microcosm images was a similarity value of 5 and a 20 pixel minimum region size value (Fig. 1.4). Having a small value for similarity was necessary to ensure that the ends of the fine roots were not classified as soil, and the minimum size of 20 was necessary to consistently separate the fine roots from the peat.

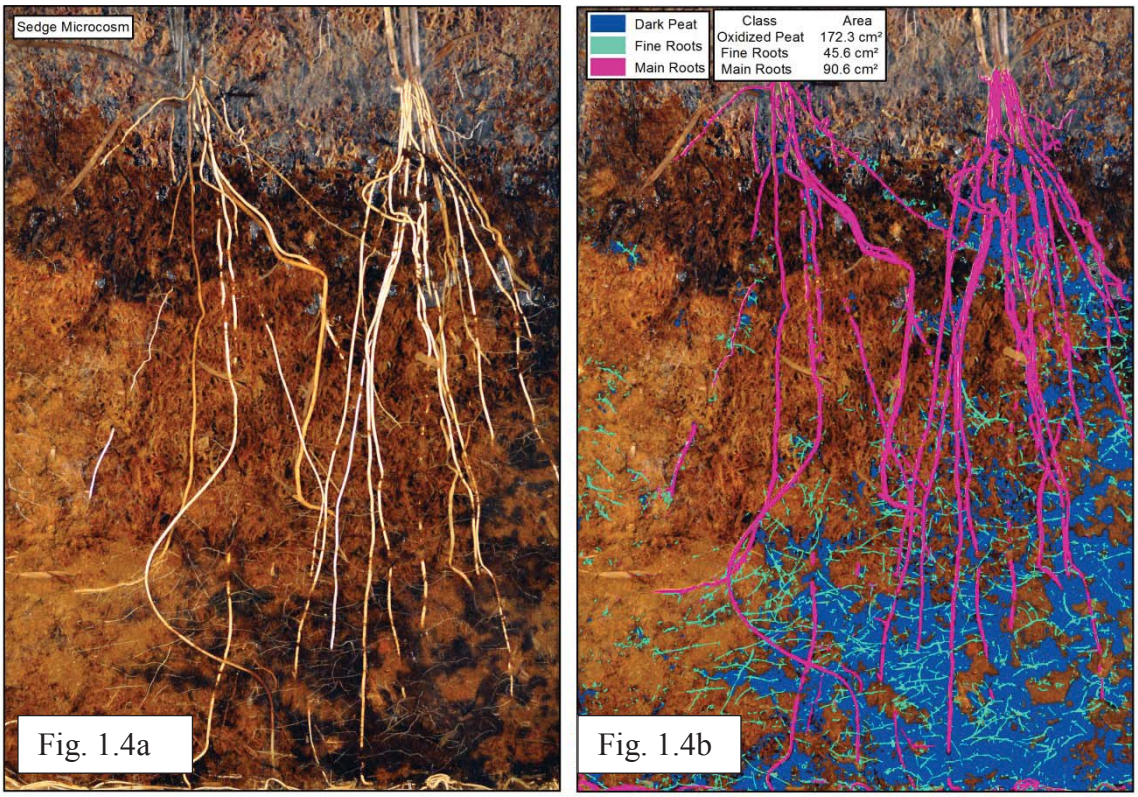

Figure 1.4 Microcosm image which has been segmented and classified: (a) microcosm image, (b) polygons produced from SPRING classification superimposed over the microcosm image.

We next analyzed mosaicked minirhizotron images using the SPRING method (Fig. 1.5). The best classification results were achieved when the images are broken into subsets, as we had issues with lighting and inconsistent settings between image frames. For the minirhizotron images, optimal similarity and minimal pixel region size varied by plant root type. Figure 1.5a is an image of a sedge (*Carex spp.)* root growing in peat with gas bubbles. Figure 1.5b displays the classification resulting from a similarity value of 20 and minimal pixel region size of 100. The minimal pixel region size of 100 proved optimal given the clear color distinction between root, gas bubbles, and peat.

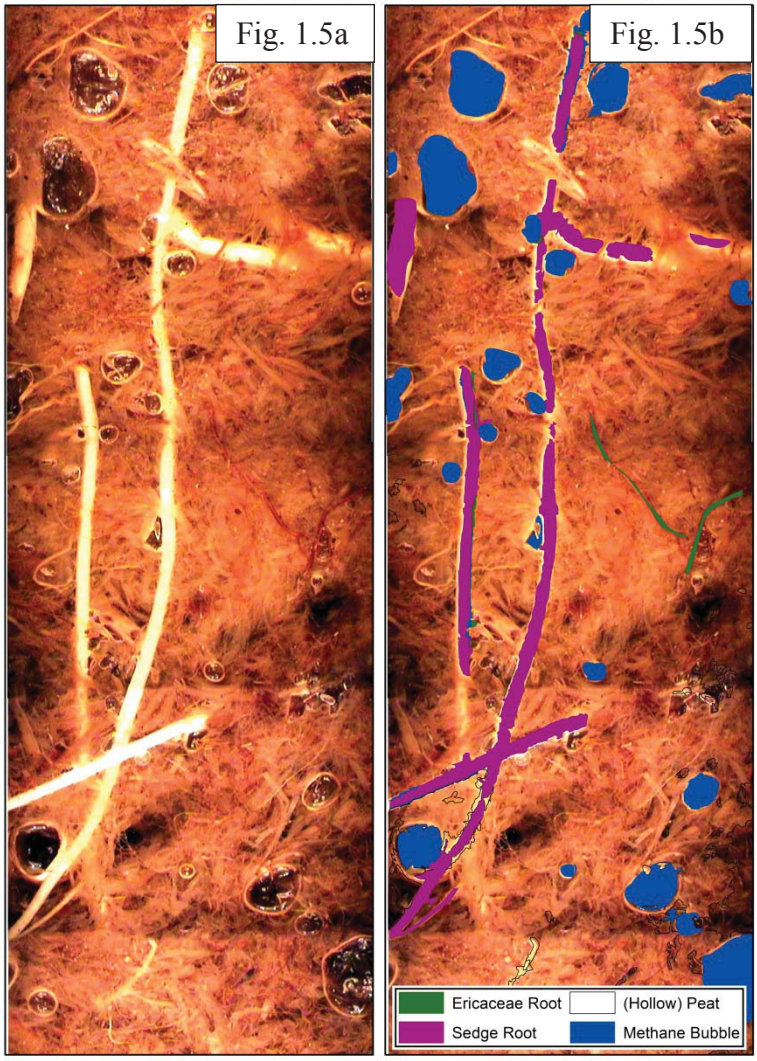

Figure 1.5 SPRING-classified mosaicked minirhizotron image: (a) the input image, (b) classification results superimposed over the image.

The second set of minirhizotron images in Figure 1.6 demonstrates the propensity of peat to shift over time, one of the unique properties of peatland soil and a significant challenge for root analyses (Iversen *et al*., 2012). To overcome this challenge SPRING was used to segment and classify the first image. The frame of a normal minirhizotron is shown in green, first position of the root is depicted in Figure 1.6a, yellow arrow. Over a month that same root has shifted out of the original frame into one below it (Fig. 1.6b,

yellow arrow), normally that would signify the disappearance of a root. With this method we are able to copy the last session's tracings and shift them down and update the shape for growth as needed, while maintaining the same identity. The attributes from each table can be subtracted one from the other to measure the growth of individual roots. This is where these methods have strengths over other programs, because we are making direct image to image comparisons.

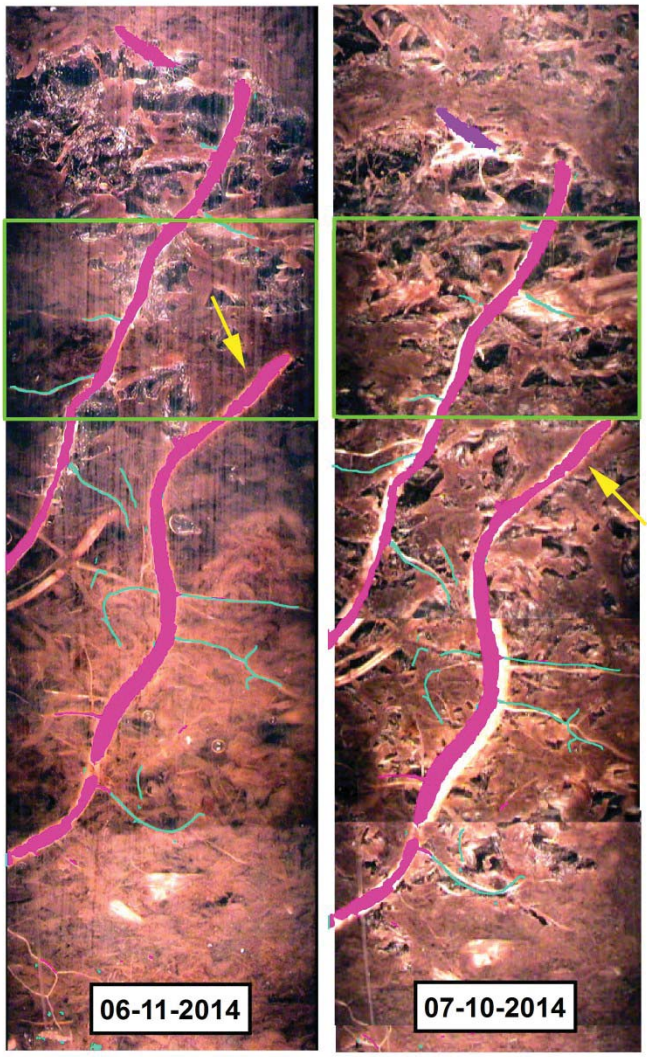

Fig. 1.6a Fig. 1.6b

Figure 1.6 SPRING-classified mosaicked minirhizotron image, green box represents the extent of a single minirhizotron image: (a) image from 6-11-2014 with the classification results superimposed over the image, (b) image from 7-10-2014 with the same classification results from 6-11-2014 superimposed over the image and shifted down with moving soil matrix.

To demonstrate the SPRING method on images from a less complex, but by no means uniform, mineral soil matrix we used rhizotron images of deciduous tree roots growing in a sandy mineral horizon (Figs. 1.7 a,b,c). These, which were collected using an infrared light source to minimize effects on roots, had segmentation performed using only the blue and green bands, because these bands displayed more contrast between soil and roots, providing better segmentation and classification results. We then performed classification and had one root class and one soil class. As in the minirhizotrons, using a larger similarity value and minimal pixel region size forced larger soil and root regions together.

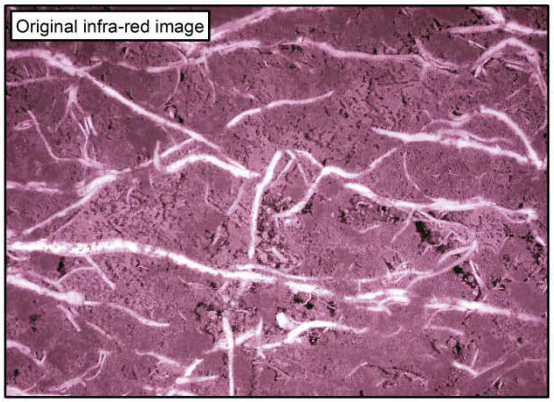

Fig. 1.7a

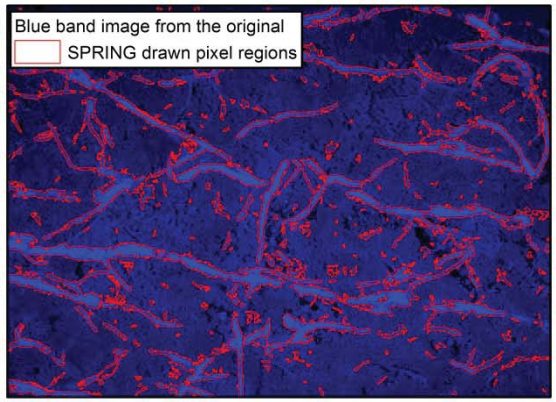

Fig. 1.7b

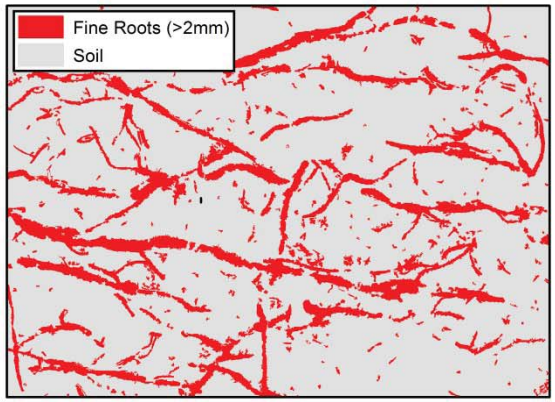

Fig. 1.7c

Figure 1.7 SPRING classified Rhizotron imagery: (a) original image, (b) pixel regions drawn only from the blue band, (c) resulting polygons from classification. Here a similarity value of 16 and a minimal pixel region size of 100 pixels were used to segment the original image.

1.3.4 *Validation of SPRING method*

To evaluate the results of our SPRING method vs. a standard hand tracing method, we took 25 images of different color and diameter string and wire overlaid on soil in microcosms (Table 1.2). These images were captured with the same camera system used for the microcosms. Images were analyzed with the SPRING method and manual vectorization using Rootfly (http://www.ces.clemson.edu/~stb/rootfly), a freely available and widely used image analysis software package. We compared root length, root diameter and image processing time in this method validation. To test the significance of the results a standardized student's t-test (α=0.05 here and throughout) in R studio environment (R Core Team, 2008) was used.

The ratio of actual length to measured lengths for both methods had a mean of 0.95 for manual tracing, and 1.02 using SPRING (Fig. 1.8a). Manual vectorizing differed from the true measurements ($t=-3.4885$, $p<0.001$, $df=24$), while the SPRING method did not ($t=1.9247$, $p=0.066$, $df=24$), indicating the SPRING method was more accurate.

Fig. 1.8a

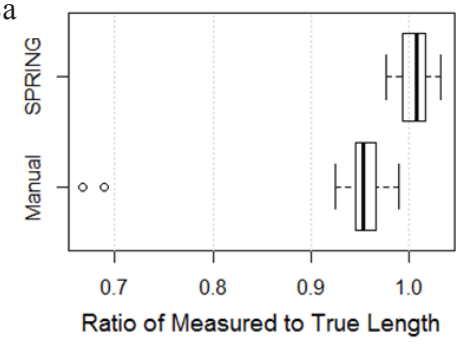

Fig. 1.8b

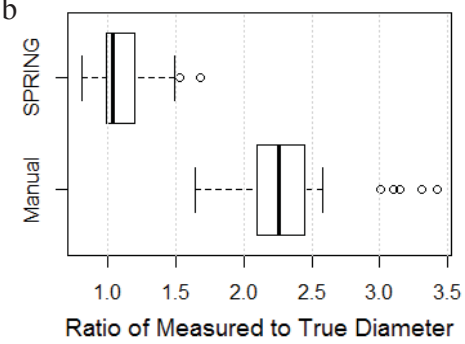

Figure 1.8 Boxplots illustrating the distribution of measured (a) length ratios and (b) diameter ratios relative to the true hand measurement using the SPRING or manual vectorization methods.

In comparing the ratios of true to measured diameters (Fig. 1.8b) we found manual tracing in Rootfly diverged from the true measurements much more than SPRING did. Manual tracing greatly overestimating diameters, with a mean ratio of 2.37 ($t=27.40$, $p< 0.001$, $df=24$). Although the SPRING method also differed significantly from the true measurements ($t=2.8753$, $p=0.008$, $df=24$), the method was much more accurate (mean ratio of 1.12). When the diameter data were broken down into color class the SPRING method produced ratios closer to one for all four test materials (Table 1.2). Interestingly, whereas in most colors both methods overestimated root diameter, brown wire diameters were underestimated by SPRING (mean ratio 0.7) and overestimated by manual tracing (mean ratio 1.53), presumably reflecting the effect of lower contrast with the soil matrix.

Table 1.2 Ratio and standard error of measured diameters to the true hand measurement using the SPRING method or manual tracing broken down by color.

			Diameter Ratio-True:Measured		*Standard error*	
"Root" material	**n**	**True diameter**	**Manual digitizing**	**SPRING & ArcMap**	**Manual digitizing**	**SPRING & ArcMap**
White string	1058	0.295 mm	1 : 3.28	1 : 1.36	0.024	0.003
White wire	353	0.813 mm	1 : 1.5	1 : 1.08	0.019	0.009
Brown wire	207	0.8 mm	1 : 1.53	1 : 0.7	0.044	0.015
Yellow wire	243	0.82 mm	1 : 1.74	1 : 0.99	0.047	0.014

In SPRING processing time did not vary significantly by root density, taking an average of 14 minutes an image, whereas processing time for manual tracing increased with complexity (8 to 39 minutes) (Table 1.3). Manual tracing had a marginally ($p<0.1$) lower processing time for low root density, marginally higher for medium root density, and significantly higher for both medium/high and high root density.

Table 1.3 Distribution of time, in minutes, to execute either the SPRING method or manual tracing according to root density (total length).

	Time (minutes)				
Length Measured (mm)	**Hand Tracing**	SD	**SPRING**	SD	*n*
1457	7.80	±0.44	11.21	±3.08	5
2501	21.17	±5.49	15.28	±1.74	6
4896	25.00	±3.53	15.38	±1.49	5
5005	31.20	±7.45	14.48	±1.20	10

To further test the accuracy of image classifications using SPRING, we used the procedure developed by Congalton & Green (1999) employing error matrices and kappa coefficients of agreement. Following their guidelines, 50 points per class were randomly placed over a classified image for each class using ArcMap, the user visually assessed the accuracy of classification, and the output was analyzed in Excel. Results showed overall classification accuracy above 90%, with a value above 80% considered to represent a very strong correlation between segmentation analysis and the true image (Landis and Koch, 1977) (Table 1.4). The Z-statistic for each image type indicated significant agreement between classified and true image (Table 1.4). The error matrix (Table S1.1) shows the instances where the sample points were classified correctly and which were most likely to be incorrectly classified.

Table 1.4 A summary table of SPRING's image classification accuracy (%), including the producer's error, user's error, overall accuracy, and the kappa coefficient of accuracy.

Photo type	Rhizotron		Minirhizotron		Microcosm	
	Producer's	User's	Producer's	User's	Producer's	User's
Main Root	93.6	88.0	100.0	96.0	86.0	95.6
Fine Root	-	-	-	-	95.5	84.0
Soil/Peat	88.7	94.0	96.2	100.0	87.7	90.9
Dark Peat	-	-			95.9	94.0
Overall accuracy	**91.0**		**98.0**		**91.0**	
Kappa statistic	**98.2**		**98.2**		**88.0**	
Z-statistic	**8.02***		**4.03***		**4.02***	

At the 95% confidance level * Significant

1.3.5 *Change detection*

Once images are acquired, change detection based on image subtraction is another possible method to quantify root demography and other belowground dynamics. Image subtraction to detect change and quantify growth is a multi-step process. In cases where the images do not overlay one another exactly, the two images must be georeferenced to one another. After georeferencing, the next step is image subtraction, then thresholding, followed by reclassification, and lastly vectorization. Image thresholding is a form of image classification based strictly on BVs and the spatial relationship between pixels is ignored. Complex change images (Fig. 1.9) can be segmented and classified using SPRING in place of thresholding and vectorization. There are two ways to perform image subtraction in ArcMap. The first way is to use ArcMap's Raster Calculator, where a single image is generated by subtracting one band from another. Alternatively ArcMap's image analysis window has a change detection tool, which generates a temporary image based on differences between images. Remote sensing image processing software such as ERDAS Imagine (Hexagon Geospatial, Norcross GA) has a change detection wizard that will produce better change analysis results than ArcMap. ERDAS Imagine allows for a change detection sensitivity adjustment, meaning it is possible to output only values that have changed by a certain percentage. If ERDAS Imagine is available, using it is strongly advised to filter out BVs indicating minor changes.

After image subtraction, image thresholding is performed in ArcMap to isolate BVs indicative of change. When the soil color does not change and the BVs are the same day to day, subtracting those pixels from another will produce no change. Soils with fluctuating color resulting from changes in moisture, disturbance, or redox reactions will

be quantified as change when using image subtraction; this can be sorted in the thresholding process. Instances of growth or root shift will be apparent in their pixel values. It is these values of no change, loss, or addition that we are classifying. The resulting raster from image subtraction will have pixel values that can be sorted into different classes in the image's symbology properties simply by sliding the break value bars over the images pixel value histogram (see supplementary protocol). Once the image pixels are sorted into different classes, the Reclassify tool can be used to create a new raster layer sorted into classes with values of 0, 1, 2, 3, etc. depending on how many classes are needed. These classes can be converted into polygons using the Raster to Polygon tool. Within this new layer's attribute table, Calculate Geometry can solve for areas of growth or change.

1.3.6 *Change detection in use*

We tested change detection in four different sets of images. The microcosm (Fig. 1.9) and mosaicked minirhizotron images (Fig. 1.10) were both processed for change detection the same way, using the image difference tool in ArcMap's Image analysis window. The microcosm image had many changing elements from week 1 (Fig. 1.9a) to week 3 (Fig. 1.9b), such as main and fine root growth and loss of peat blackening (Fig. 1.9c). We found classification and segmentation of the change detection image in SPRING, rather than thresholding, to produce the best results (Fig. 1.9d). The resulting polygons of SPRING segmentation and classification were used to calculate new root growth and loss of peat blackening (Fig. 1.9d).

Fig. 1.9a Fig. 1.9b Fig. 1.9c Fig. 1.9d

Figure 1.9 Microcosm change analyses: (a) microcosm image from week1, (b) microcosm image from week 3, (c) results of change analysis (the black color represents new root growth, the dark gray represents loss of oxidation zones, and the light blues represent constant), (d) results from segmentation and classification in SPRING enabling the calculation of growth and loss

Two different sets of minirhizotron images were analyzed with change detection. The first example (Fig. 1.10) demonstrates the change detection method in a minirhizotron environment. Minor peat shifts from month to month were corrected with georeferencing prior to change detection; however major shifts in soil matrix may not permit georeferencing as the distortion could be too great. Change detection was performed on the blue bands from week 1 (Fig. 1.10a) and week 4 (Fig. 1.10b). The appearance of a new root is displayed in black (Fig. 1.10c) in the resulting image. To extract the values associated with the new root, the image underwent thresholding, reclassification, and raster to polygon conversion. Following conversion the resulting new root polygon was selected and exported to produce its own layer (Fig. 1.10d). If there were multiple new roots or any other new phenomena of interest those polygons could be selected and made into a layer as well.

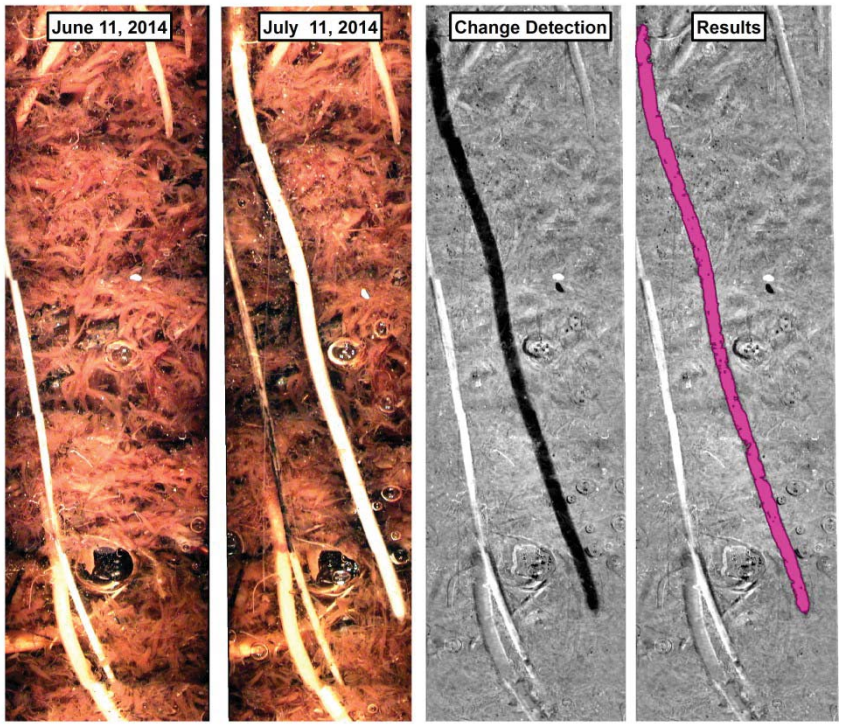

Fig. 1.10a Fig. 1.10b Fig. 1.10c Fig. 1.10d

Figure 1.10 Minirhizotron change analysis II root and peat displacement: (a) week one imagery, (b) week 4 imagery, (c) results from thresholding change analysis.

Using rhizotron imagery, we performed change detection on a series of 17 images of a mycorrhizal fungal hyphal fan to observe change over time (Fig. 1.11). This fan displayed remarkable growth from week 1 (Fig. 1.11a) to week 26 (Fig. 1.11b). We used ArcMap's Raster Calculator to execute image subtraction in the blue band, as it had the most contrast between hyphae and soil. Within ArcMap's Raster Calculator tool we selected week n and subtracted it from the week n-1 image. Image subtraction, thresholding, reclassification, and vectorization resulted in polygons delineating growth at approximately biweekly intervals. These polygons were stacked over one another (Fig. 1.11c) to display growth dynamics. The polygons all have a known area that can be used to quantify growth.

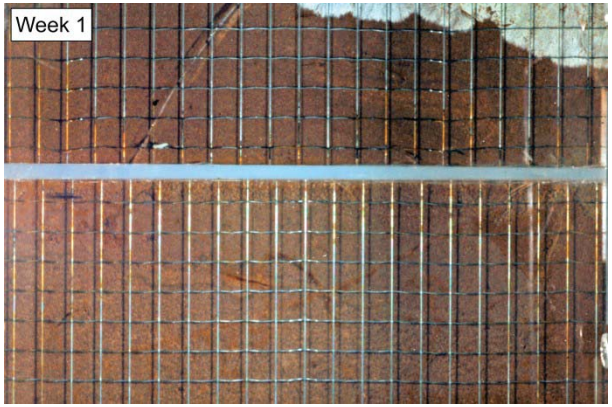

Fig. 1.11a

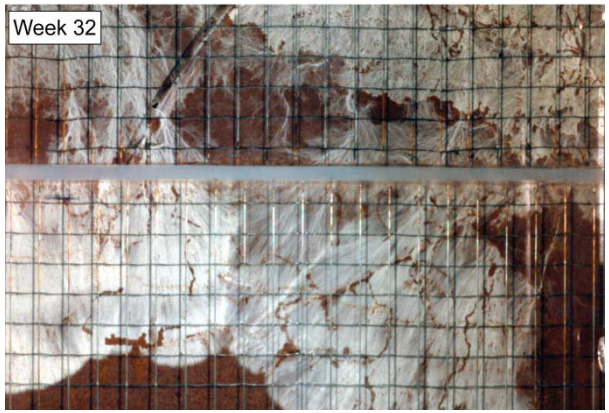

Fig. 1.11b

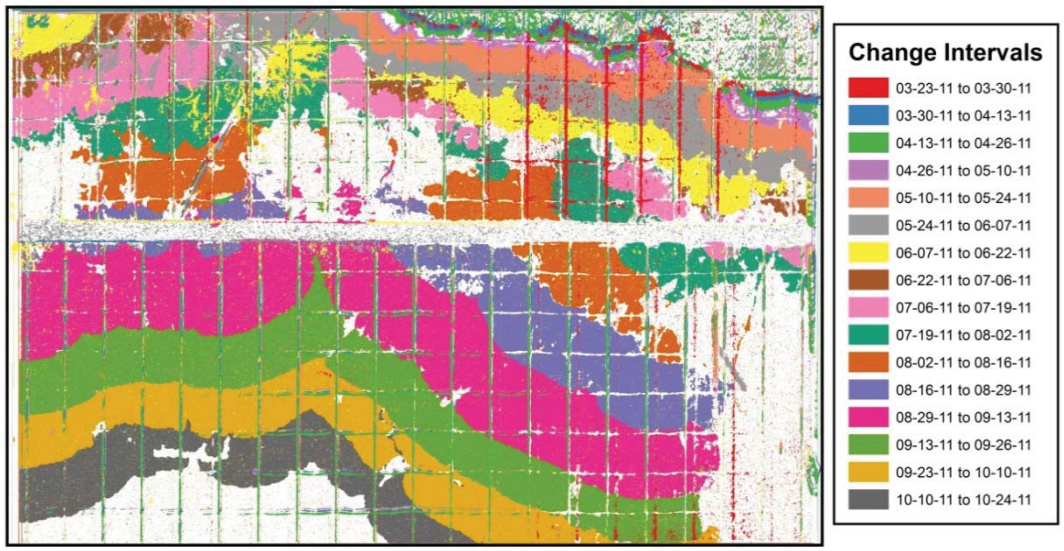

Fig. 1.11c

Figure 1.11 Rhizotron change analysis, (a) week one imagery, (b) week 32 imagery, (c) extracted pixel BV's which indicated growth. Each ribbon of color on the figure represents 32 weeks of bi-weekly interval of hyphae growth.

1.3.7 *ArcMap Spatial Analysis of classified or change detection imagery*

Spatial analysis is the final step following segmentation and classification in SPRING or change detection. Either method results in polygons with their own identities. The first step in spatial analysis is determining the spatial scale (see Supplemental protocol). Once the scale is known, area and perimeter of each polygon can be calculated automatically in the ArcMap attribute table using Calculate Geometry, then rescaled. Object (root, soil patch, worm burrow, etc.) diameters and lengths are also calculated automatically with Vectorization (see Supplemental protocol). With the Field Calculator any equation for further quantitative analysis can be entered, such as surface area or volumes. The Summarize Tool in the attribute table will generate statistics on total lengths for each field or areas (see Supplemental protocol).

In ArcMap there is access to additional functions that can enhance the image analysis of these complex soil environments. With the Measure Tool we are able to generate exact measurements of root depth in minirhizotron tubes. With the Identify Cursor, we are able to obtain true color values for each band. In addition, fields can be created in the attribute table for additional root data (e.g., branching order, species). Chemical analysis from points of interest could be performed and imported into ArcMap as point data, allowing an in-depth spatial study of biogeochemical processes in the rhizosphere. ArcMap also has a powerful suite of spatial statistics tools allowing the user to measure relationships between sets of data, thus integrating data processing and statistical analysis.

Concluding remarks

The application of our approaches to image analysis can enhance understanding of belowground ecosystem processes. Our appended protocols, combined with basic training in GIS methods, permit application of our methods in complex soil matrices. With the use of these methods we were able to delineate areas of roots, mycorrhizal hyphae, soil redox, and gas bubbles from imagery in a natural environment.

Our semi-automated methodologies clearly outperformed manual-tracing methods of vectorization in both time and accuracy. With increasing root density, processing time did not increase and accuracy did not decrease. In imagery where soil matrix and roots had good color distinction it was easy for SPRING to accurately differentiate and classify relevant features. The greatest challenge for all methods, including ours, is areas of low contrast between matrix and object of interest.

These methods proved to be capable of processing large sets of complex data rapidly. Working with SPRING's image segmentation and classification algorithms in conjunction with ArcMap users can employ readily available powerful semi-automated tracing algorithms, within a user-friendly program where coding with is not required. Errors from SPRING are also easily corrected in ArcMap's point-and-click environment.

Mosaicking minirhizotron images together for analysis was advantageous in terms of processing time, as well as for dealing with shifting positions of roots in peat over time. With one consecutive image we were easily able to observe and note large root displacement, especially when displacement was along the vertical axis. This is impossible for unmosaicked images.

In conclusion, our methodologies permit root demographic analysis of more complex images than standard root analysis methods, as well as belowground image analysis beyond root demographics. By facilitating application of GIS and remote sensing image processing technologies in this novel arena we expect to enhance the rate of scientific progress in belowground ecosystem research.

1.5 References

Bins LS, Fonseca LM G, Erthal G J, Ii FM 1996. Satellite imagery segmentation: a region growing approach. *Simpósio Brasileiro de Sensoriamento Remoto* **8**: 677-680.

Câmara G, Souza RCM, Freitas U M, Garrido J. 1996. SPRING: Integrating remote sensing and GIS by object-oriented data modelling. *Computers & graphics **20***: 395-403.

Chapin FS, and Ruess RW . 2001. Carbon cycle: The roots of the matter. *Nature* **411**: 749-752.

Christensen, PB, Revsbech, N P, Jensen, KS. 1994. Microsensor analysis of oxygen in the rhizosphere of the aquatic macrophyte Littorella uniflora (L.) Ascherson. *Plant Physiology* **105**: 847-852.

Congalton RG, Green K. 1999. Assessing the accuracy of remotely sensed data: principles and practices. Lewis Publishers. *New York*: **137**.

Downie HF, Adu MO, Schmidt S, Otten W, Dupuy LX, White PJ, Valentine TA. 2014. Challenges and opportunities for quantifying roots and rhizosphere interactions through imaging and image analysis. Plant, cell & environment.

ESRI (Environmental Systems Resource Institute). 2014. ArcGIS Desktop: Release 10.1. Redlands, CA: Environmental Systems Research Institute.

Farrar JF, Jones DL. 2000. The control of carbon acquisition by roots. *New Phytologist **147***, 43-53.

French A, Ubeda-Tomás S, Holman T J, Bennett MJ, Pridmore T. 2009. High-throughput quantification of root growth using a novel image-analysis tool. *Plant physiology* ***150*****:** 1784-1795.

Gasch CK, Collier TR, Enloe SF, Prager SD. 2011. A GIS-based method for the analysis of digital rhizotron images. Plant Root 5, 69–78.

Gijsenij A, Lu R, Gevers T. 2012. Color constancy for multiple light sources. *Image Processing, IEEE Transactions on* ***21***, 697-707.

Iversen C M, Murphy MT, Allen MF, Childs J, Eissenstat DM, Lilleskov EA, Sullivan PF. 2012. Advancing the use of minirhizotrons in wetlands. *Plant and soil*, ***352***: 23-39.

Jackson R, Moone, HA, Schulze ED. 1997. A global budget for fine root biomass, surface area, and nutrient contents. *Proceedings of the National Academy of Sciences* **94:** 7362-7366.

Johnson JF, Allmaras RR, Reicosky DC. 2006. Estimating source carbon from crop residues, roots and rhizodeposits using the national grain-yield database. *Agronomy journal* ***98***. 622-636.

Landis JR, Koch GG. 1977. The measurement of observer agreement for categorical data. *Biometrics*: 159-174.

Majdi H. 1996. Root sampling methods-applications and limitations of the minirhizotron technique. *Plant and Soil*, ***185***(2): 255-258.

Milchunas DG. 2009. "Estimating root production: comparison of 11 methods in shortgrass steppe and review of biases." *Ecosystems* **12**: 1381-1402.

Persichetti P, Simone P, Langella M, Marangi GF, Carusi C. 2007. "Digital photography in plastic surgery: how to achieve reasonable standardization outside a photographic studio." *Aesthetic plastic surgery*, **31***:* 194-200.

Pierret A, Moran CJ, Doussan C. 2005. "Conventional detection methodology is limiting our ability to understand the roles and functions of fine roots." *New Phytologist*, **166**: 967-980.

Plataniotis KN, Venetsanopoulos AN. 2000. Color image processing and applications. Springer.

Plourde L, Congalton RG. 2003. Sampling method and sample placement: how do they affect the accuracy of remotely sensed maps. *Photogrammetric Engineering and Remote Sensing* **69**: 289-297.

R Development Core Team. 2008. R: A language and environment for statistical computing. R Foundation for Statistical Computing, Vienna, Austria. ISBN 3-900051-07-0, URL http://www.R-project.org.

Rasse DP, Rumpel C, Dignac MF. 2005. Is soil carbon mostly root carbon? Mechanisms for a specific stabilisation. *Plant and soil* **269**: 341-356.

Rewald B, Ephrath JE. 2012. Minirhizotron technique. *Plant roots: the hidden half, 4th edn. CRC Press, New York*.

Rossner M, Yamada KM. 2004. What's in a picture? The temptation of image manipulation. *The Journal of Cell Biology* **166**: 11-15.

Schmidt MW, Torn MS, Abiven S, Dittmar T, Guggenberger G, Janssens IJ, Kleber M, et al. 2011. Persistence of soil organic matter as an ecosystem property. *Nature* **478**: 49-56.

Shojaedini SV, Heidari M. 2013. A New Method for Root Detection in Minirhizotron Images: Hypothesis Testing Based on Entropy-based Geometric Level Set Decision. *International Journal of Engineering* **1:** 1.

Singh A. **1989**. Review Article Digital change detection techniques using remotely-sensed data. *International Journal of Remote Sensing* **10**: 989-1003.

Smithwick EA, Lucash MS, McCormack ML, Sivandran G. 2014. Improving the representation of roots in terrestrial models. *Ecological Modelling* **291**: 193-204.

Taylor BN, Beidler KV, Strand AE, Pritchard SG. 2014. Improved scaling of minirhizotron data using an empirically-derived depth of field and correcting for the underestimation of root diameters. *Plant and Soil* **374**: 941-948.

Trumbore S, Da Costa ES, Nepstad DC, Barbosa De Camargo P, Martinelli LA, Ray D, Silver W. 2006. Dynamics of fine root carbon in Amazonian tropical ecosystems and the contribution of roots to soil respiration. *Global Change Biology* **12**: 217-229.

Wan S, Norby RJ, Pregitzer KS, Ledford J, O'Neil EG. 2004. CO_2 enrichment and warming of the atmosphere enhance both productivity and mortality of maple tree fine roots. *New Phytologist* **162**: 437-446.

Vamerali T, Bandiera M, and Mosca G. 2012. Minirhizotrons in modern root studies. *Measuring roots*. Springer Berlin Heidelberg: 341-361.

Veresoglou SD, Chen B, Rillig MC. 2012. Arbuscular mycorrhiza and soil nitrogen cycling. *Soil Biology and Biochemistry **46*:** 53-62.

Zeng G, Birchfield ST, Wells CE. 2008. Automatic discrimination of fine roots in minirhizotron images. *New Phytologist* **177**: 549-557.

Zeng G, Birchfield ST, Wells CE 2010. Rapid automated detection of roots in minirhizotron images. *Machine Vision and Applications* **21**: 309-317.

1.6 Appendix A

Table of Contents:

Giving images a false coordinate system

Images are giving a false coordinate system using the Define Projection tool, found in the Data Management Projections and Transformations Toolbox in ArcMap. A UTM projection is needed so the images sit on a flat grid, we used NAD 83 UTM Zone 16N. Define Projection does not create a new image, it provides the images real coordinates. These coordinates will give each pixel a resolution or 1 meter, so rescaling is simple.

If there are many images to give a projection to, use the Model Builder for batch processing. In place of using the Define Projection command for each image individual a model can be created which will repeat the command for each image automatically. Creating this model (Fig. S1.1) is done by opening a new model. Then insert→ iterators →Rasters, from here drag and drop a file on the Iterate Rasters hexagon, select workspace or catalog. If there is a folder with multiple subfolders containing images that need a projection, then double click on the iterate rasters hexagon, and select recursive. Selecting recursive enables ArcMap to go through all of the subfolders and define the projection for every image. After that bring the define projection tool into the model by selecting it from the toolbox and dragging it into the model, then selecting the UTM projection. Then press play (Fig. S1.1, red arrow).

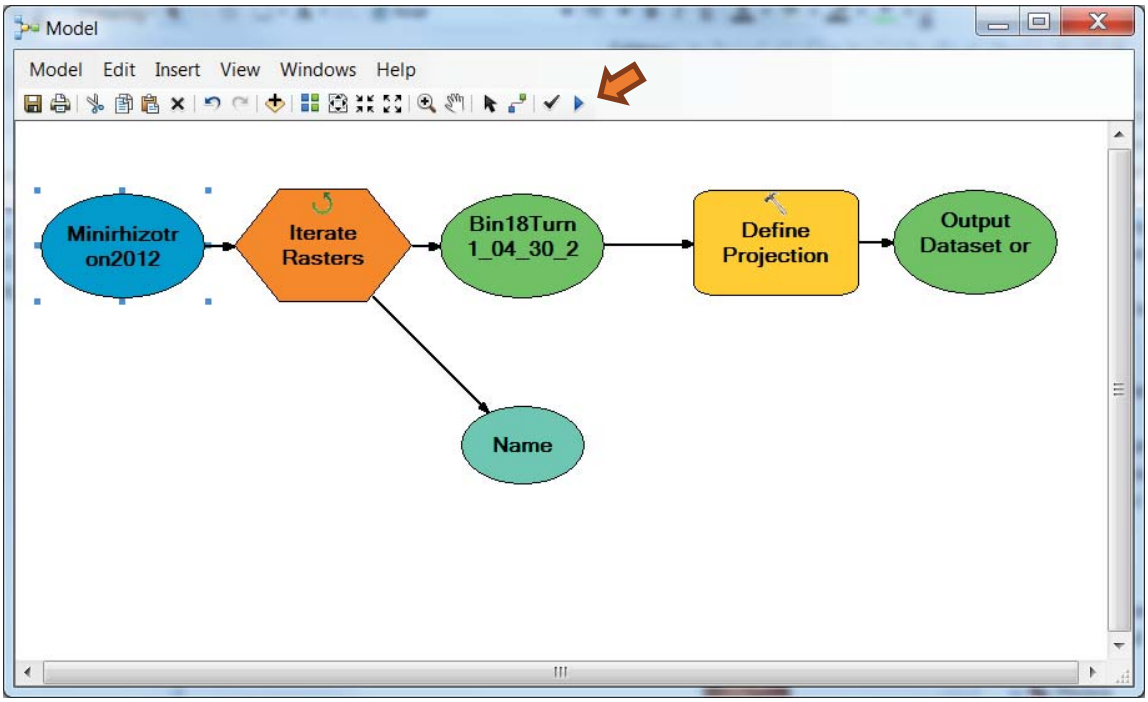

Figure S1.1 Example of a model for defining projections in ArcMap.

Spatial resolution calculations

To solve for image spatial resolution use an image a ruler or any object with a known measurement. Give the image a false X, Y coordinate system. Images with a UTM coordinate system have each pixel representing 1 meter. So any measurement made in ArcMap can then be scaled appropriately easily. Zoom in as close to the imaged ruler as possible to count how many pixels make up one millimeter (could use centimeters or nanometers). Divide the known length by the number of pixels spanned to solve for the length of one side of a pixel, this will provide the **rescaling factor**. For example, one millimeter on a ruler could span 10 pixels, which means each pixel is equal to 0.1 mm.
Within the attribute table create a new field for length and use calculate geometry to solve for area of all root segments. Then create another field length_scaled type equals float, to rescale the results within the attribute table using the field calculator. Within the field calculator select [length] and multiply it by the rescaling factor.

*Calculate geometry and field calculator are found by right clicking on the field title within the attribute table.

SPRING flowchart

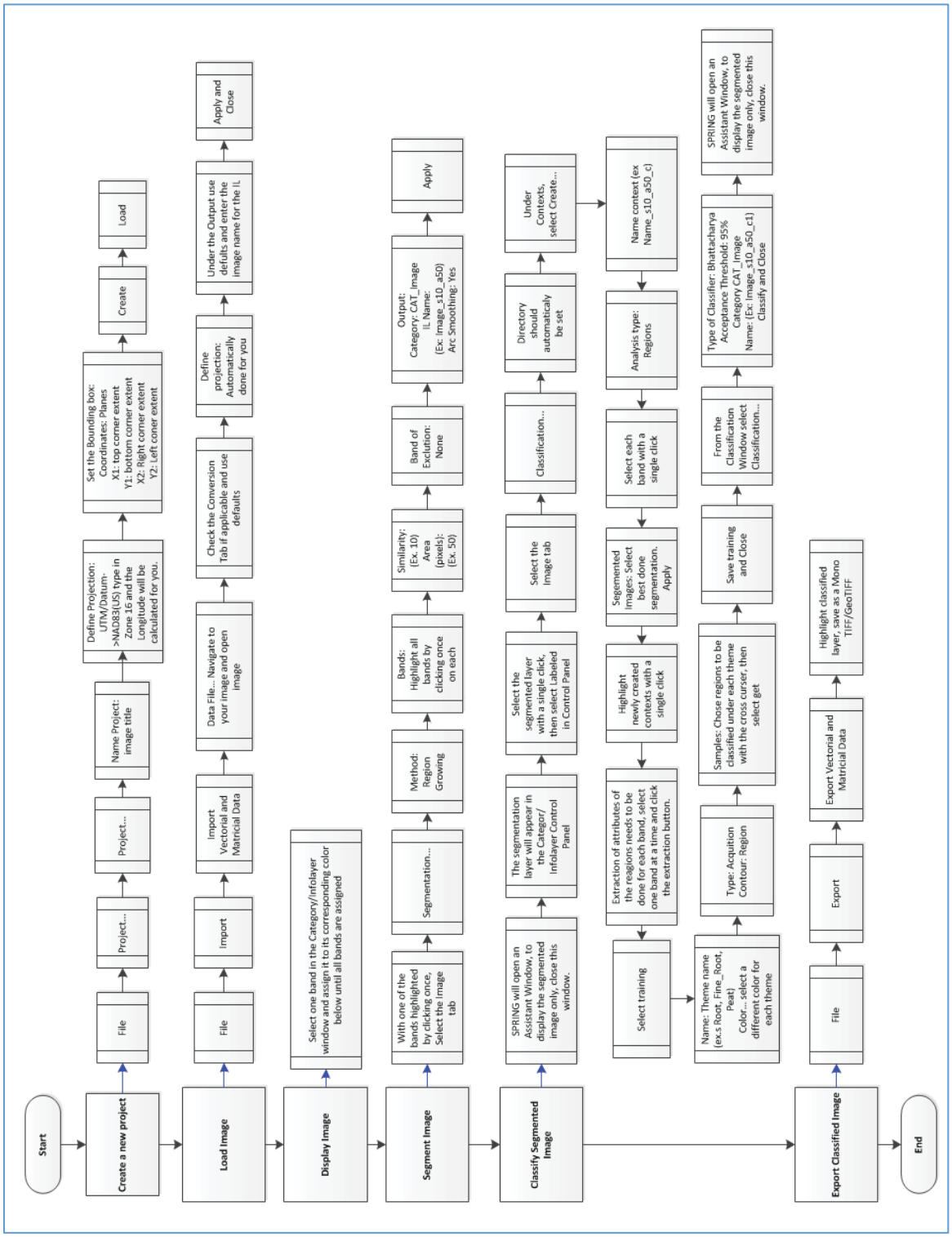

Figure S1.2 Steps taken to segment and classify an image in SPRING. The main steps are bold in text on the left. The blue arrows off the main steps are instruction to complete these steps.

Post SPRING Analysis

Following SPRING Classification each image has to be converted to a Polygon layer, see section *Converting SPRING imagery*. After converting to a polygon the next step is dependent on your question, if only interested in areas, ArcMap calculates those automatically, see sections *Editing classification errors in ArcMap,* then *Spatial resolution calculations,* and *Calculating areas and a building a richer dataset.* If lengths and diameters are needed see sections: *Thresholding, Vectorization and Raster Editing,* then *Calculating areas and a building a richer dataset.*

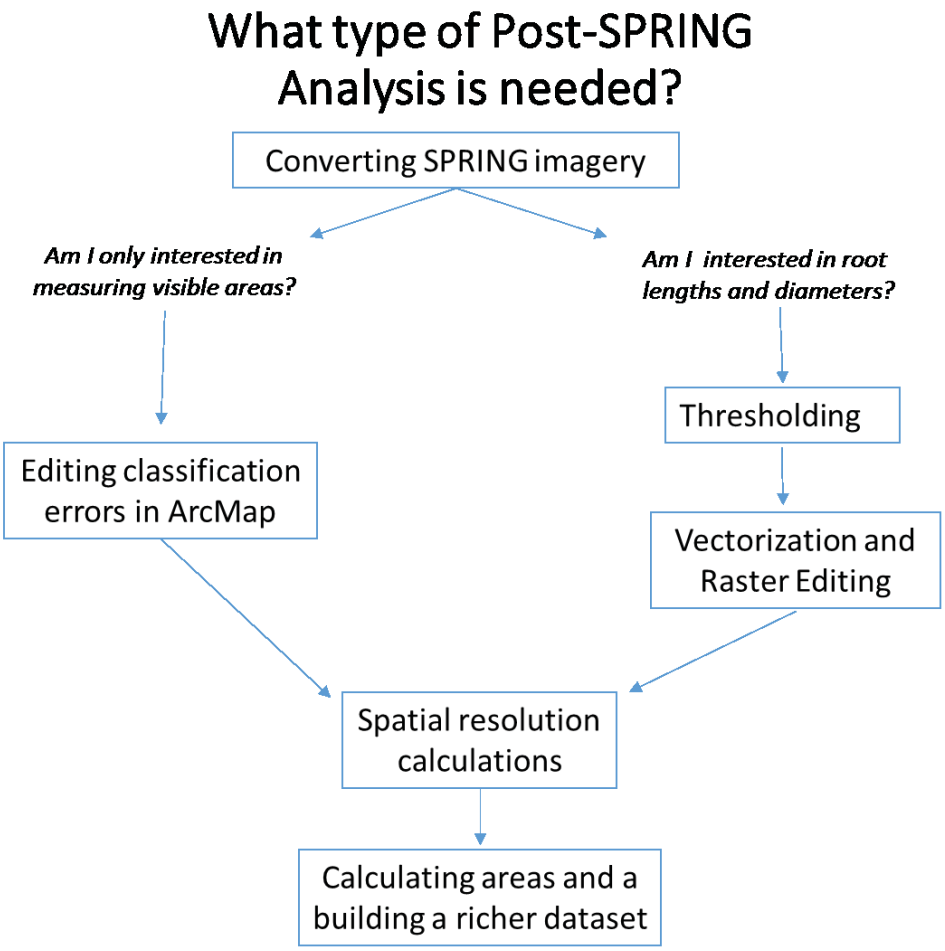

Figure S1.3 Post-SPRING analysis steps.

Converting SPRING imagery

Once there is a classified image exported out of SPRING, export the original image as well. Instead of exporting as a Mono like with the classified image, export as RBG and fill each RBG Chanel with the associated band (Fig. S1.4). By exporting both images, realignment by georeferencing in ArcMap is avoided and the original and classified image will line up perfectly. Once both images are exported, use the Conversion tool > From Raster > Raster to polygon, this step is used to maintain the grid codes from SPRING indicating type and will allow us to edit errors in classification if any.

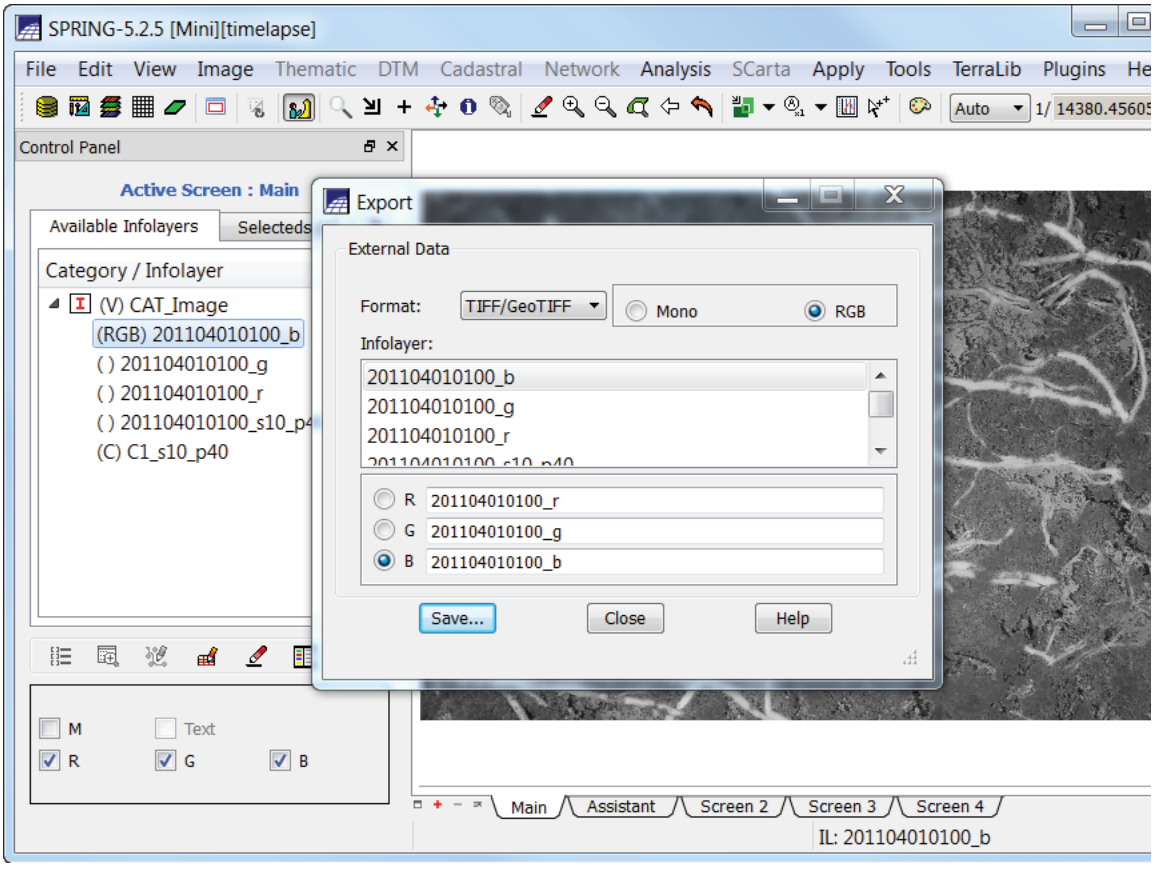

Figure S1.4 Example of exporting an image from SPRING.

Editing classification errors in ArcMap

Once there is a polygon version of a classified image and an exported original image, minor classification errors can be corrected. First display the polygon layer by the GRIDCODE using symbology. Then begin an editing session. Editing is best taught with ArcMaps tutorial found here:

http://resources.arcgis.com/en/help/main/10.1/index.html#//01m500000003000000

After editing move onto *Spatial Resolution Calculations* and then *Calculating areas and a building a richer dataset*.

Thresholding

Thresholding is the act of grouping pixels together based on their brightness value. To do this in ArcMap start with either a SPRING classified image (used for this demonstration) or an image produced from change analysis. First start by displaying the image from the Catalog into the Table of Contents (Fig. S1.5). The values displayed are classes defined in SPRING. The values under the 0-1 layer class represent soil and colored light green. Layer classes 1-5 are roots and are colored red or yellow and the 0 class (dark green) are values that were not classified. The image following (Fig. S1.5) had one soil class, an unclassified layer and 4 root classes; these are the values to be used for thresholding.

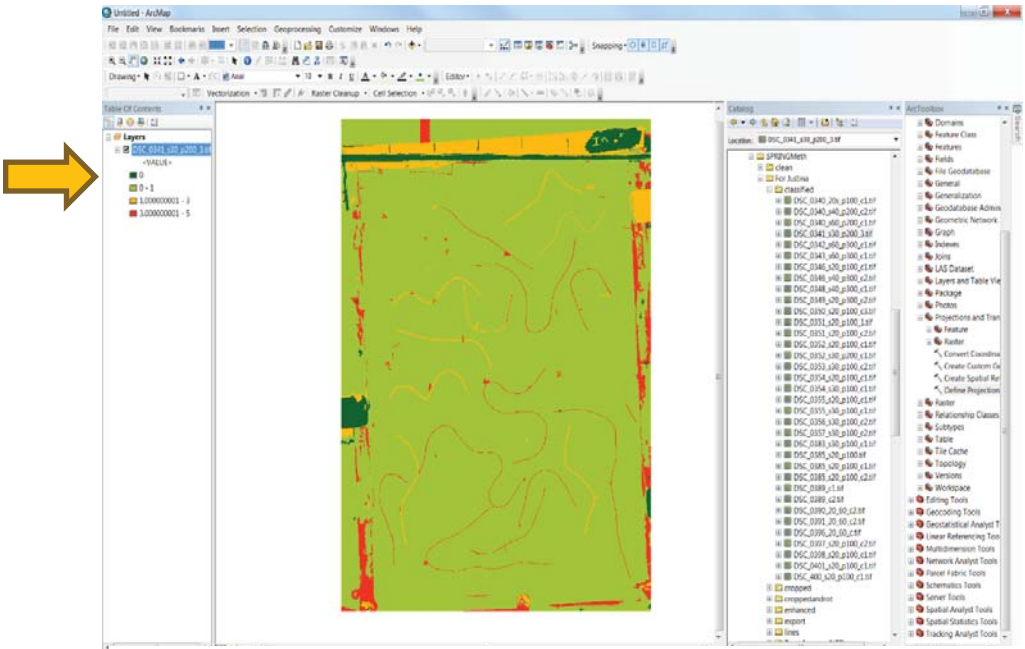

Figure S1.5 The results of SPRING classification displayed in ArcMap.

The next step is to assign threshold classifications: click on the name of the image (Fig. S1.5, purple arrow) > select layer properties; this window will open (Fig. S1.6, blue arrow) > select the Symbology tab > Show > Classified (Fig. S1.6, red arrow). Then click on Classify (Fig. S1.6, orange arrow), the Classification window will appear (Fig. S1.6, green arrow). From here choose 2 classes as Vectorization requires a raster symbolized with 2 colors. The break values for this example will be 1.0 and 5, values between 1 and 5 are roots and between 0 and .999999 are soil.

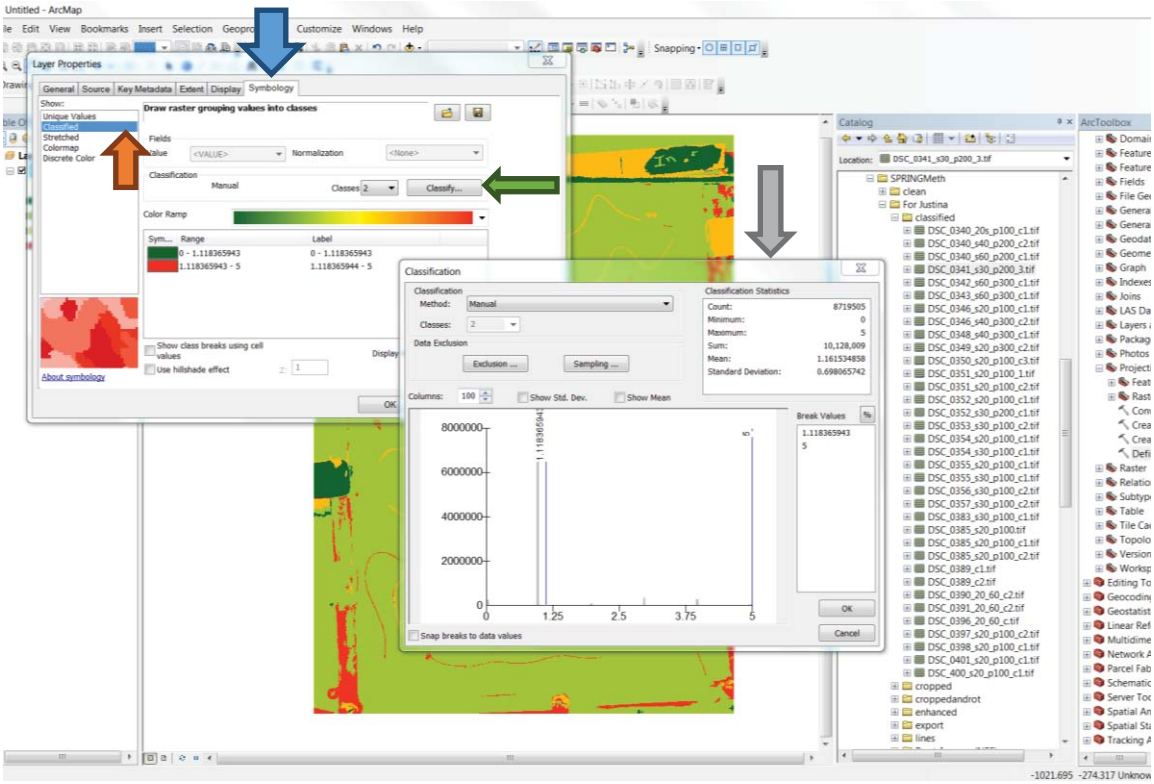

Figure S1.6 Example of layer properties symbology and classification.

Once the values are changed, use the reclassify tool to create a new layer with two classes- root and background. The final reclassified image should like Figure S1.7.

Then move on to *Vectorization and Raster editing* on the next page**.**

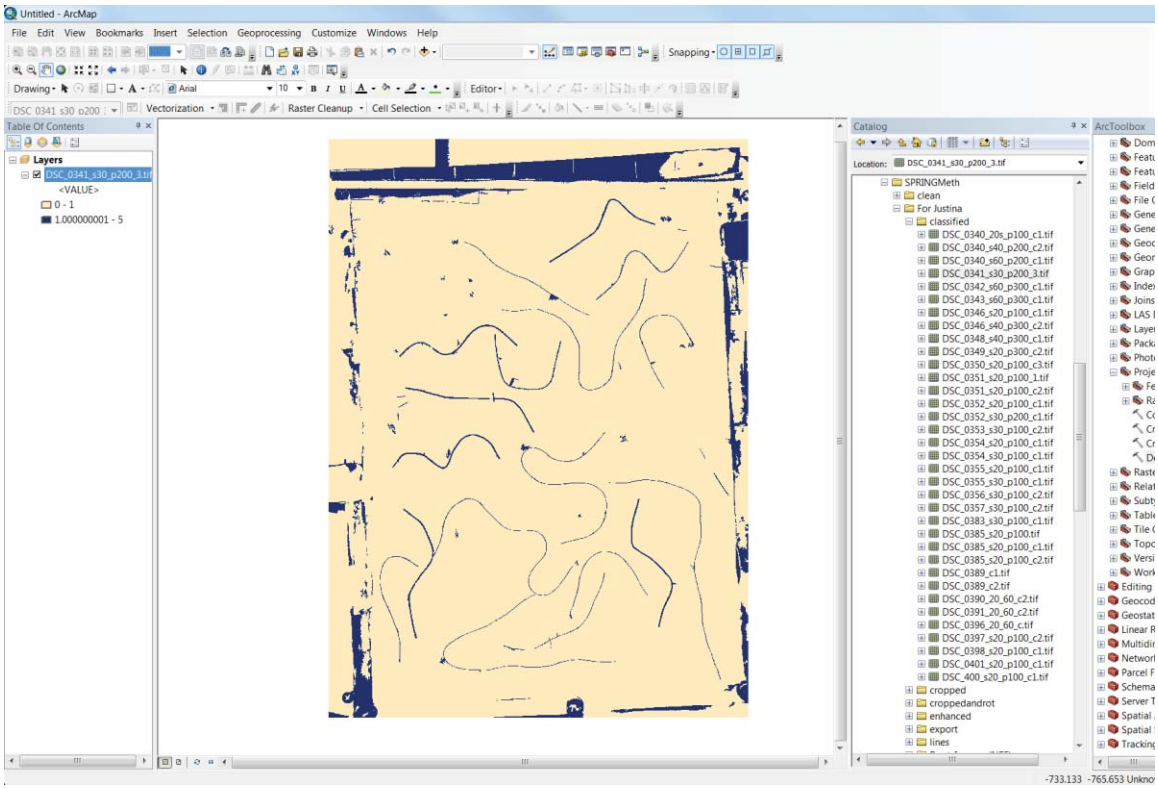

Figure S1.7 Reclassified image.

Vectorization and raster editing

To automatically measure for lengths and diameters of roots,use the ArcScan extension. Within the ArcScan extension is the Vectorization tool Generate Feature, which enables automated tracing. Follow the steps under **Thresholding in ArcMap** first. Once there is a reclassified layer with apparent root and soil zones use ArcScan's Raster Cleanup to fix any errors. In Figure S8 below we see an area of soil that is being classified as root (green arrow). To fix this begin with turning on the editor. First go to Customize > Toolbars > and check Editor, it should appear (red arrow). Left click on Editor > Start Editing, select the image which needs to be edited. Then turn on ArcScan Customize > Extensions > ArcScan; once the ArcScan extension (blue arrow) is turned on, add the toolbar to the display Customize > Toolbars > and check ArcScan, then under Raster Cleanup select Start Clean up. Within the ArcScan Toolbar turn on Raster Painting, Raster Clean up > Select Raster painting toolbar and it will appear (purple arrow). The steps to turn on the Editor, ArcScan, and Raster Painting should only need to be done once, then every time ArcMap is started the Editor should appear automatically.

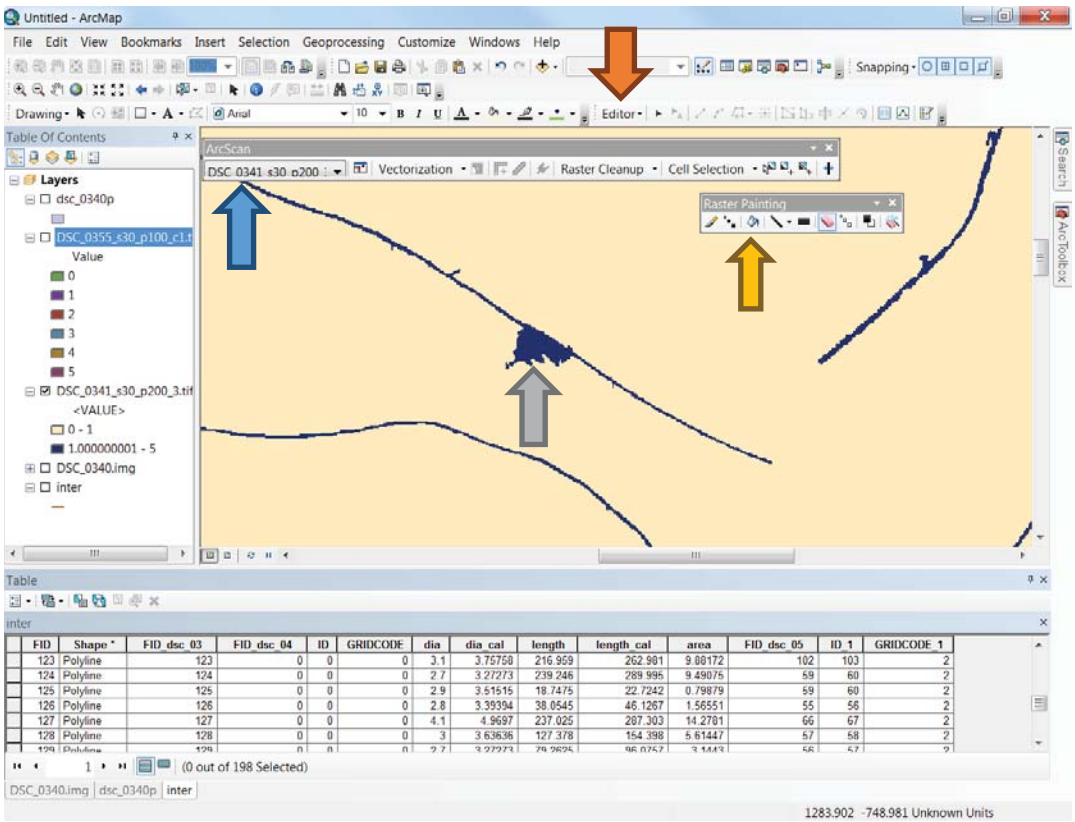

Figure S1.8 Using raster cleanup to fix errors from segmentation and classification.

Next, the eraser can be used to erase the small area of soil (Fig. S1.9). This is also where missing roots can be drawn in with the paint brush. The Magic Erase Tool can be used to erase entire segments, as displayed on the next page (Fig. S1.11 before editing and Fig. S1.12 after editing). A great trick for this kind of editing is to make the soil layer hollow, and add the original image behind it. In Figure S1.10 there is a bit of root that was left behind in classification, it can easily be "painted" back in.

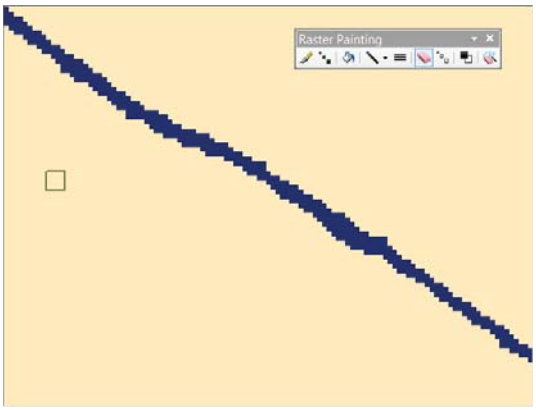

Figure S1.9 Edited root segment

Figure S1.10 Missing end of a root after segmentation and classification.

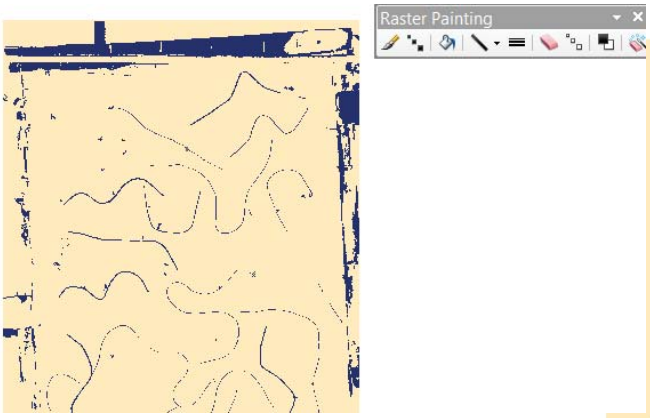

Figure S1.11: Reclassified segmented and classified image before editing.

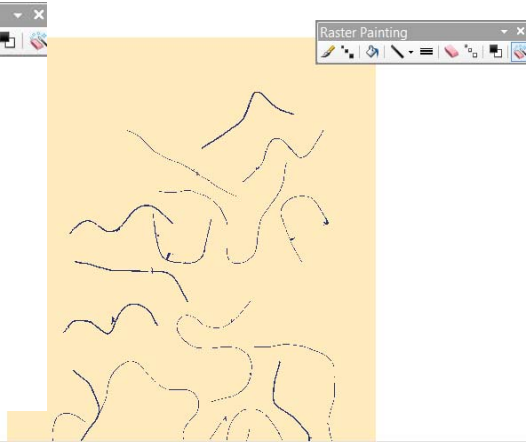

Figure S1.12 Same image from Figure 11 after editing.

Once the classified raster's representation of the image is satisfactory, go to the editor, save all edits and stop editing. The next step is to convert the raster to a polygon again; this polygon layer will only have two grid codes, which is needed for Vectorization. Convert the second polygon layer to a polyline layer ArcToolbox > Data Management Rools > Features > Feature to Line. To the new polyline layer add a field to the attribute table named diameter and set the type as a float. Resumeediting and select the polyline layer, go to Vectorization > Generate Features, and match the Generate Features window to Figure S1.13. Select okay, the tool will create new features and they will be highlighted in cyan. These features need to be made into their own layer, as right now they are a part of the polyline layer. By right clicking on the polyline layer in the table of contents > Data> Export Data, save this layer in a Vectorized folder. Then use the Define Projection command again on the Vectorized layer and the first polygon layer.

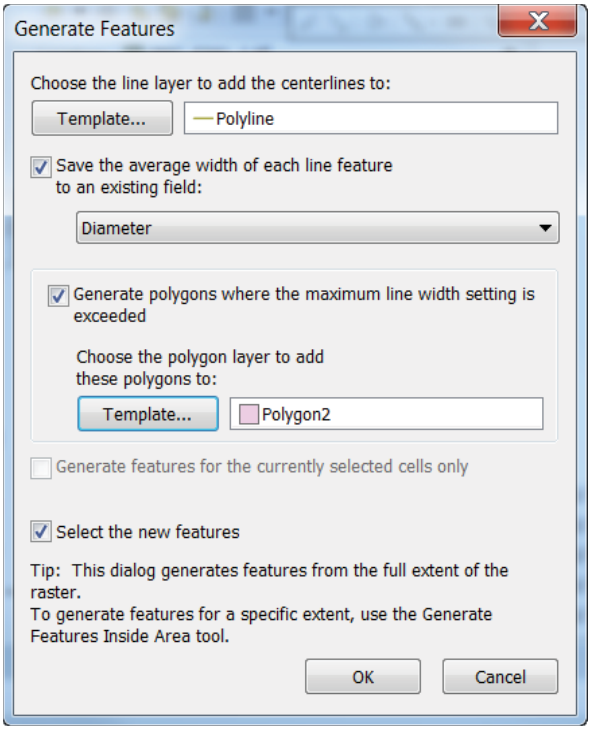

Figure S1.13 Generate features

Calculating areas and a building a richer dataset

Following change analysis, SPRING classifiction or Vectorization, the analysis of resulting measurements can be made. Any additionally needed fields can also be added to the attribute table such as: length, length to scale, diameter and area to scale, depth, or color. Fields are added by selecting Table options > Add Field in the attribute table. Field types for numerical values should be designated as floatsand any notes should be designated as text fields. Length and areas are calculated automatically with Calculate Geometry. Use the Field Calculator to scale automatically calculated lengths and areas down. Use Statistics to find the sum, average, or min, and max values of each field. Field Calculator, Calculate Geometry, and Statistics are all found by right clicking on the name of a field (Figure S1.14). Use the measure tool (Fig. S1.15, blue arrow) to generate manually measured diameters and rooting depth (remember 1 meter with a UTM coordinate systems equals 1 pixel). Use the identify cursor (Fig. S1.15, red arrow) to find the red, green, and blue values.

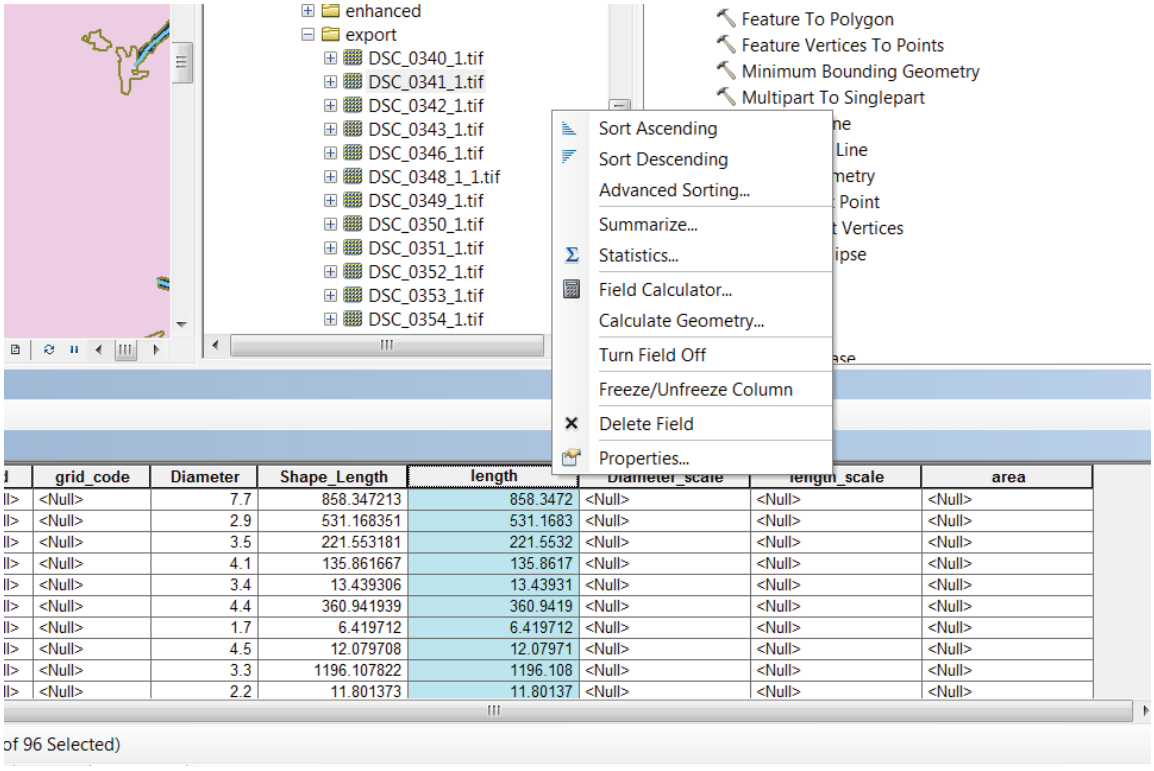

Figure S1.14 Using Field Calculator, Calculate Geometry, or Statistics in an example attribute table.

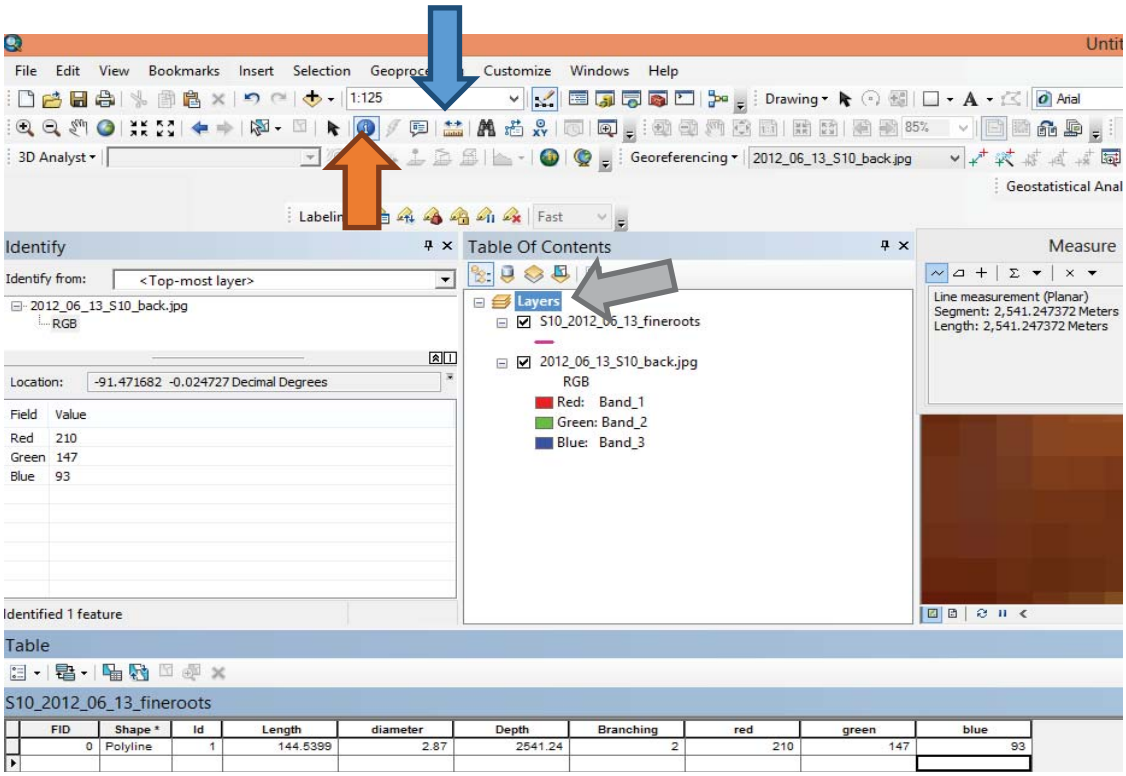

Figure S1.15 Location of the Identify and Measure tool and display of the Identify window.

Note: If the measure tool is grayed out, right click on Layers (Fig. S1.15, green arrow), select Properties…, then Coordinate System, and select the coordinate system being used as the false coordinate system.

**If there is interest in the classes established in SPRING, use the intersect tool, Geoprocessing > Intersect (Figure S1.16). To intersect the vectorized layer ranked 1 and the polygon1 layer ranked 2. This will add the grid codes to the vectorized layer. The new layer will now have a series of grid codes (root type class from SPRING), lengths, and diameters for each root individually.

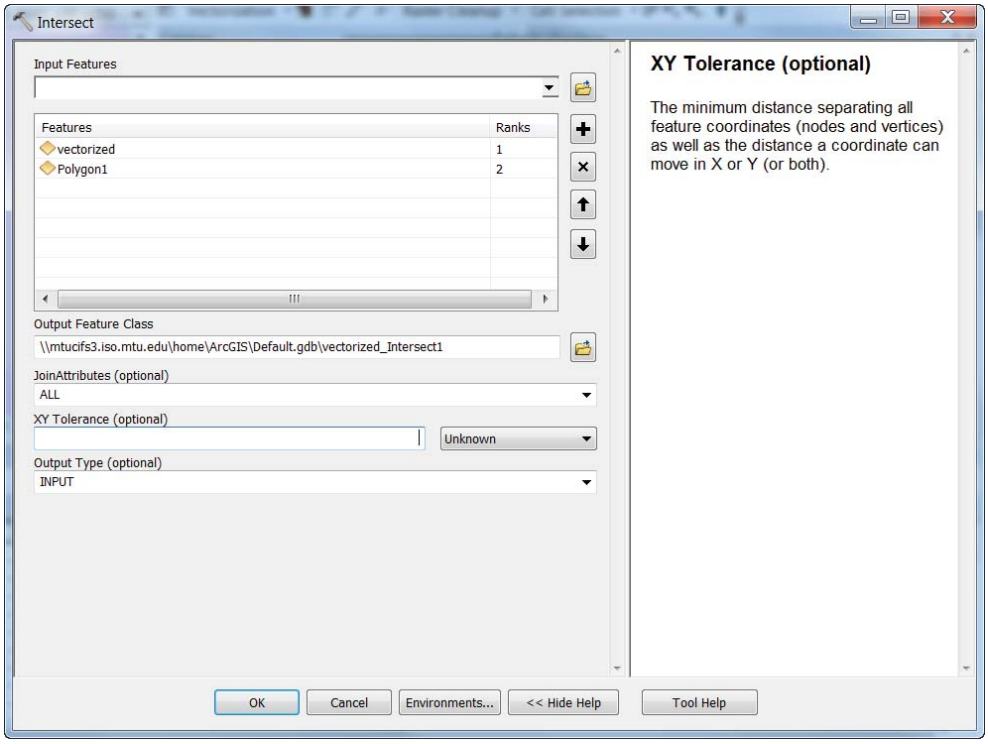

Figure S1.16 Intersect tool interface

Manually digitizing roots in ArcMap

In overly complex root systems, manual digitizing could still be the best method for analysis. Using ArcMap for tracing roots by hand is simple and easier to work with them programs specifically designed for roots.

Step one: Make a blank feature class.

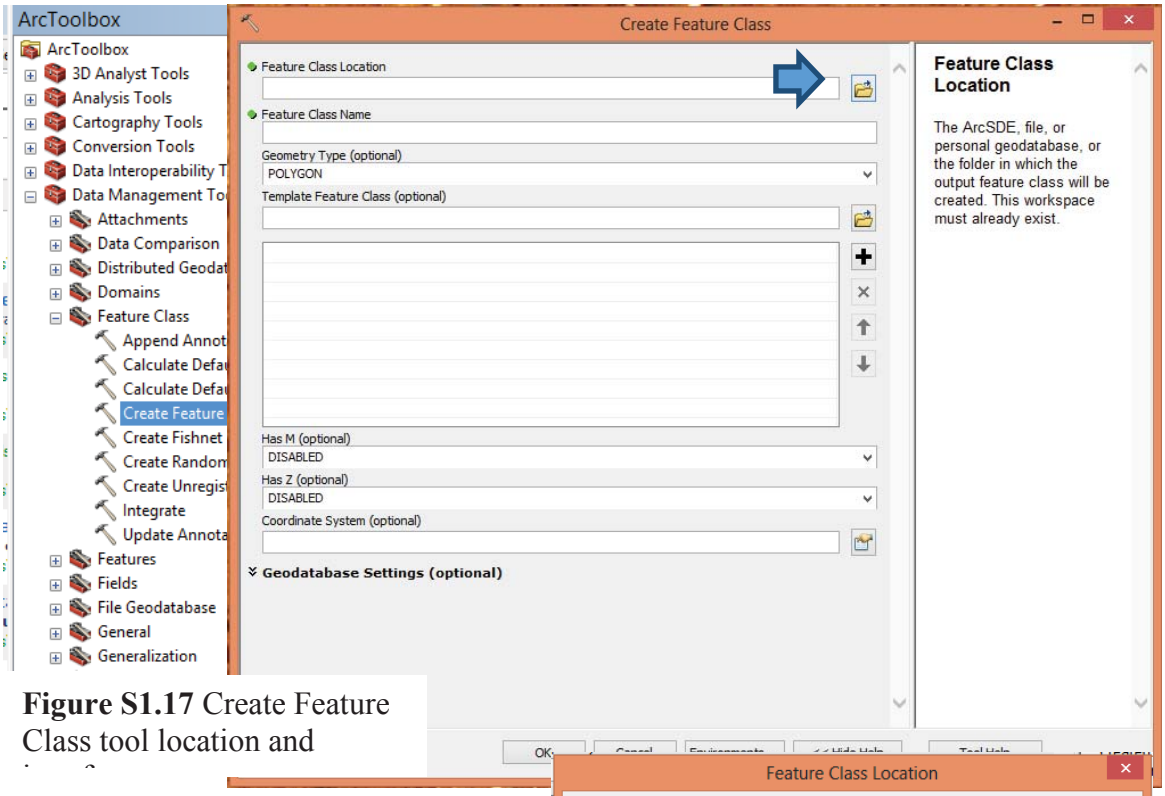

Figure S1.17 Create Feature Class tool location and

Figure S1.18 Example of how to enter the Feature Class Location.

In ArcToolbox>Data Management Tools>Feature Class>Create Feature Class (Fig. S1.17). Once within the tool, the first required input is a folder for the new feature class. Select the map to folder button (Fig. S1.17 blue arrow), navigate to the location to save the digitized root layers, and create a new folder in this location. Once a new folder is created, select it with a single left click. The name should appear (Fig. S1.18, red arrow).

Then next input is name of the feature class, in this case fine roots, which will be namedS10_2012_06_13_fineroots (no spaces) (Fig. S1.19). The geometry type will be a polyline, as it will be traced along the center of root. The last input is a coordinate system; any UTM coordinate system can be used. Leave the rest of the input options as the default.

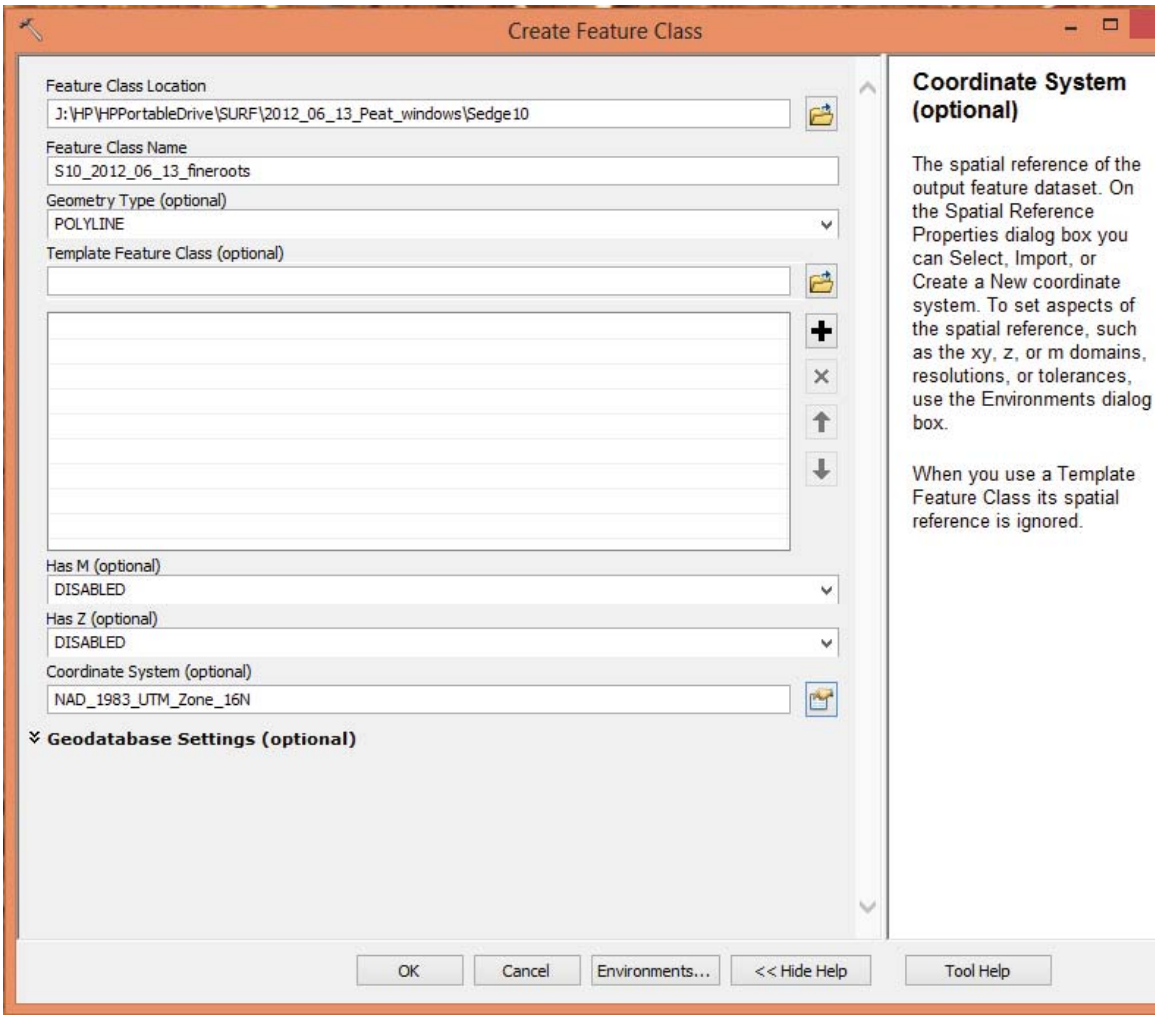

Fig. S1.19: Example of the Create Feature Class interfaced with all required inputs.

Add the new feature class to the ArcMap Table of Contents. From here additional columns can be added to the attribute table for additional required data (lengths, colors, depths, etc.). Open the attribute table. Then add a field, for example length and make it a float. Fields can also be created for diameter, root depth, branching order, and red, green, blue values, and these will all be designated as float type. The resulting attribute table should look something like Figure S1.20.

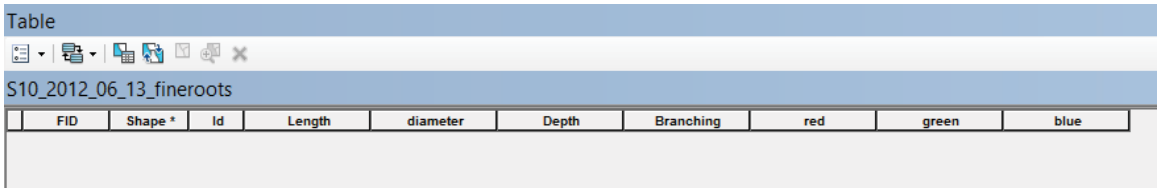

Figure S1.20 Example of a detailed attribute table.

Step two: Digitize roots.

Go to the editor toolbar and select start editing. Once editing is started, go back into the Editor toolbar>Editing Windows>Create Features (Fig. S1.21). This will bring up the create features window (Fig. S1.22). Select the blank feature class with a single left click to activate the construction tools.

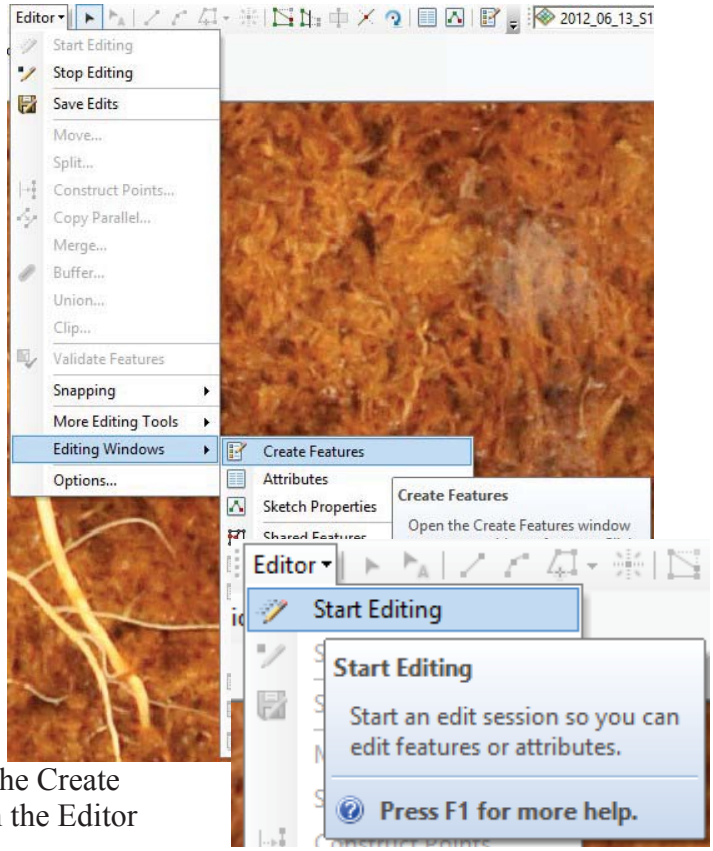

Figure S1.21 Location of the Create Features editing window in the Editor

Use either the line or freehand tool to draw a center line through the root. The freehand tool will enables the user to draw a curved line by single clicking the starting point and then the ending point (Fig. S1.22, green arrow). The line feature will require multiple clicks along the root, then a double click to end the line (Fig. S1.23, purple arrow).

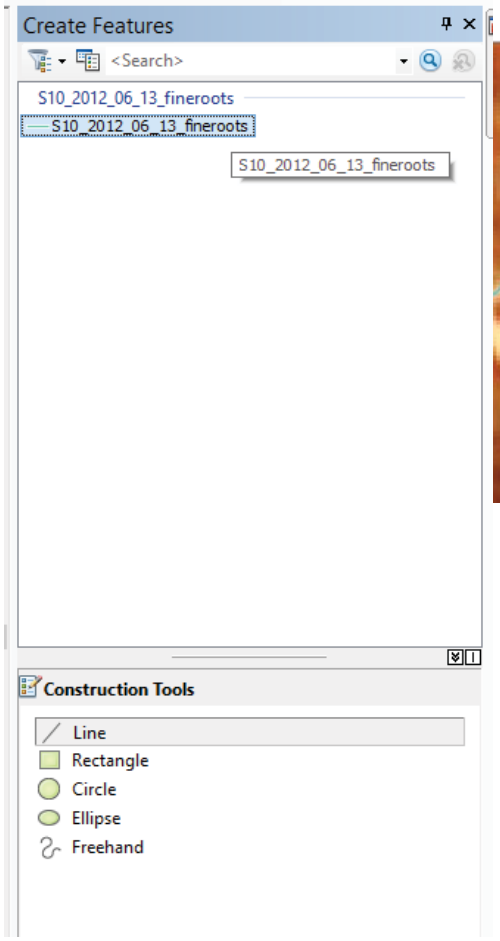

Figure S1.22: Create Features editing

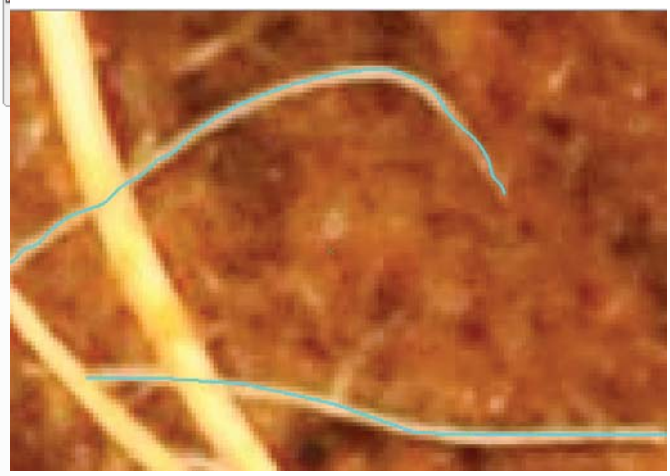

Figure S1.23 Vectorizing roots.

After a root vector is created, additional information can be added to the attribute table pertaining to that root segment (see **Calculating areas and building a richer data set).**

Save edits often and when finished select Stop editing from the editor toolbar. Lastly, rescale the data by adding two new fields one for the true length and one for true diameter.Use the Field Calculator to multiply length and/or diameter by the rescaling factor.

When solving for lengths over consecutive dates , and there is a need to alter the tracing from the a previous date's image, simply right click and copy the feature class from the table of contents in ArcMap, and paste into a new location. Rename the feature class by right clicking and selecting rename. Begin a new editing session and change to locations or lengths. Legth and diameter will need to be re-calculated and rescaled once finished altering the tracing.

***Potential Issue: The Halo effect**- Reflection from the root to the glass adding a "glow" around the root. In the Figure S1.24 example, it is known that this root is truly 3 μm in diameter, not 5.29 μm. From a distance (Fig. S1.24) you cannot tell there is a reflection off the root to the glass, but when zoomed in you can see pixels that are very white and pixels that are tan/gray in color (Fig. S1.25), which demonstrates the importance of working at the pixel level,. Keep this in mind when looking at vectorization results, and if during segmentation the halo was included in your results, you will want to scale the measurements down. Further work in the development of an algorithm to mask the halo around a root is needed. This could be a cause in overestimation in many root tracing systems.

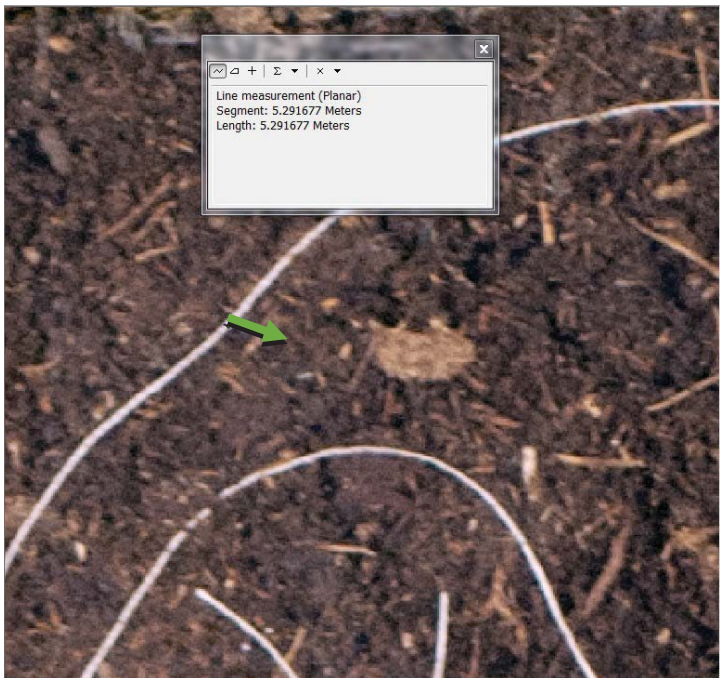

Figure S1.24 Image of roots where the diameter is measured from a far (not at pixel level).

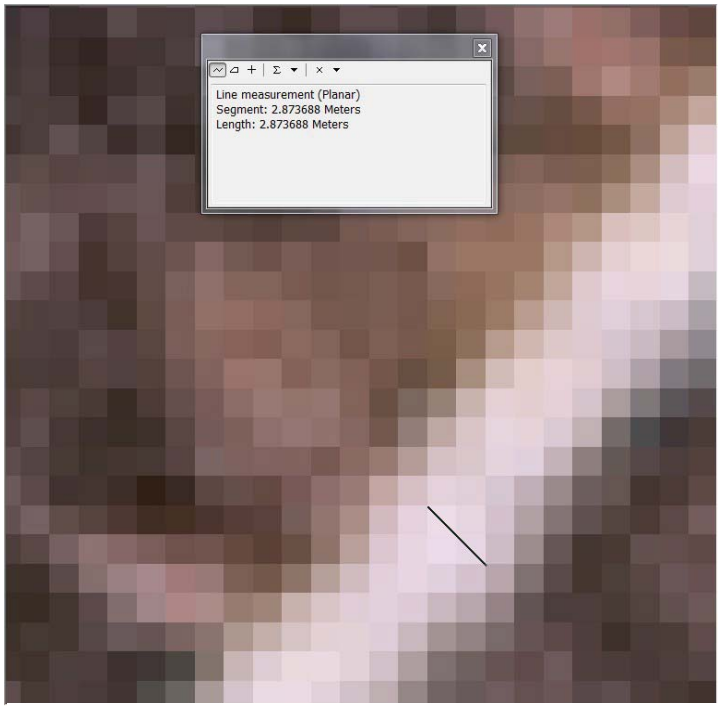

Figure S1.25 Image of root where the diameter measurement is acquired at the pixel level.

Saving imagery

Image compression should never be used when saving images. Compression algorithms eliminate redundant information for storage, once displayed again the image might look fine at full scale, but when zoomed to the pixel level there is a significant difference in quality. A loss of detail at the pixel level is significant when imaging roots that are originally only a pixel or two wide. Compression also leads to changes in color, which is important to consider if measuring colors. Images should always be stored as an uncompressed .tiff or .img; compressed formats such as a .jpg should be avoided.

*Try it out- Save a RAW image as a.jpg and as a .tiff and zoom in to both levels. Try different levels of JPEG compression. There will be a noticeable difference at the pixel level.

1.2 Supplementary Material:

Table S1.1: The error matrix demonstrates SPRING's ability to segment and classify and image accurately, it is produced by randomly testing 50 points per image classification and comparing SPRING classification to the true class.

Rhizotron			
	Root	Soil	Row Total
Root	**44**	6	50
Soil	3	**47**	50
Column Total	47	53	**100**

Minirhizotron			
	Root	Soil	Row Total
Root	**48**	2	50
Soil	0	**50**	50
Column Total	48	52	**100**

Microcosm					
	Root	Fine Root	Peat	Dark Peat	Row Total
Root	**43**	1	0	1	45
Fine Root	2	**42**	5	1	50
Peat	5	0	**50**	0	55
Dark Peat	0	1	2	**47**	50
Column Total	50	44	57	49	**200**

1.7 Appendix B

```
# Code that automates stitching together minirhizotron images

import arcpy
import os
import sys
from arcpy.sa import *

from arcpy import env

# Set the current workspace

env.workspace=
"I:/Mesocosm/QAQCimages/Minirhizotron2011/July2011/Bin01_08032011/Turn2"
maindir = str(env.workspace)

rasterList = arcpy.ListRasters()
for raster in rasterList:
   print raster

#Define projection
for raster in arcpy.ListRasters():
        #print raster
        arcpy.DefineProjection_management(raster,
"PROJCS['NAD_1983_UTM_Zone_16N',GEOGCS['GCS_North_American_1983',DAT
UM['D_North_American_1983',SPHEROID['GRS_1980',6378137.0,298.257222101]],P
RIMEM['Greenwich',0.0],UNIT['Degree',0.0174532925199433]],PROJECTION['Transv
erse_Mercator'],PARAMETER['False_Easting',500000.0],PARAMETER['False_Northin
g',0.0],PARAMETER['Central_Meridian',-
87.0],PARAMETER['Scale_Factor',0.9996],PARAMETER['Latitude_Of_Origin',0.0],U
NIT['Meter',1.0]]")
        #print "defined projection for" + str(raster)

#Clip rasters and create a new folder in the dirctory for them to go

cropped_newpath = str(maindir) + "/" + "cropped"
if not os.path.exists(cropped_newpath): os.makedirs(cropped_newpath)

##Clip Raster Dataset by known extent - Left Bottom Right Top

env.workspace= maindir
outputworkspace= cropped_newpath
rasterList = arcpy.ListRasters()
for raster in arcpy.ListRasters():
```

```
    raster1=str(outputworkspace) + "/" + str(raster[:-4])
    arcpy.Clip_management(raster, "-0.5 -520.5 729.5 -7.5", str(raster1 + ".img"))

#Create file for shifted images

shift_newpath = str(maindir) + "/" + "shiftimages"
if not os.path.exists(shift_newpath): os.makedirs(shift_newpath)

#Shift images

env.workspace= cropped_newpath
outputworkspace= shift_newpath
xdir=1
float(xdir)
xinc=1
float(xinc)
ydir=-485
float(ydir)
yinc=-485
float(yinc)
rasterList = arcpy.ListRasters()
for raster in arcpy.ListRasters():
    print raster
    raster2=str(outputworkspace) + "/" + str(raster[:-4])
    arcpy.Shift_management(raster, str(raster2 + ".img"), xdir, ydir)
    xdir= xdir+xinc
    ydir= ydir+yinc


#Create folder for mosiac image

final_newpath = str(maindir) + "/" + "finalimage"
if not os.path.exists(final_newpath): os.makedirs(final_newpath)

#Mosiac images

env.workspace= shift_newpath
outputworkspace= final_newpath
rasterList = arcpy.ListRasters()

# Set local variables
outname = "Tube1_T2_Bin1BDate08_03_11.gdb"

# Execute CreateFileGDB
GDB = arcpy.CreateFileGDB_management(outputworkspace, outname)
```

```
gdbname = GDB
mdname = "MosiacDataset"
prj =
"PROJCS['NAD_1983_UTM_Zone_16N',GEOGCS['GCS_North_American_1983',DAT
UM['D_North_American_1983',SPHEROID['GRS_1980',6378137.0,298.257222101]],P
RIMEM['Greenwich',0.0],UNIT['Degree',0.0174532925199433]],PROJECTION['Transv
erse_Mercator'],PARAMETER['False_Easting',500000.0],PARAMETER['False_Northin
g',0.0],PARAMETER['Central_Meridian',-
87.0],PARAMETER['Scale_Factor',0.9996],PARAMETER['Latitude_Of_Origin',0.0],U
NIT['Meter',1.0]]"
noband = "3"
pixtype = "8_BIT_UNSIGNED"
pdef = "NONE"
wavelength = ""

mosaic_dataset = arcpy.CreateMosaicDataset_management(gdbname, mdname, prj,
noband, pixtype, pdef, wavelength)


#Add Raster Dataset type Raster to FGDB Mosaic Dataset
#Calculate Cell Size Ranges and Build Boundary
#Build Overviews for Mosaic Dataset upon the 3rd level Raster Dataset pyramid
#Apply TIFF file filter
#Build Pyramids for the source datasets

mdname = mosaic_dataset
rastype = "Raster Dataset"
inpath = shift_newpath
updatecs = "UPDATE_CELL_SIZES"
updatebnd = "UPDATE_BOUNDARY"
updateovr = "UPDATE_OVERVIEWS"
maxlevel = ""
maxcs = "#"
maxdim = "#"
spatialref = "#"
inputdatafilter = "*.img"
subfolder = "NO_SUBFOLDERS"
duplicate = "EXCLUDE_DUPLICATES"
buildpy = "NO_PYRAMIDS"
calcstats = "CALCULATE_STATISTICS"
buildthumb = "NO_THUMBNAILS"
comments = "Add Raster Datasets"
forcesr = "#"
```

```
Mosiac = arcpy.AddRastersToMosaicDataset_management(mdname,  rastype, inpath,
updatecs, updatebnd, updateovr,maxlevel, maxcs, maxdim, spatialref,
inputdatafilter,subfolder, duplicate, buildpy, calcstats, buildthumb, comments, forcesr)

#Set mosiac dataset properties

Mosiac2 =
arcpy.SetMosaicDatasetProperties_management(Mosiac,"","","","None","","","","NOT_
CLIP","FOOTPRINTS_MAY_CONTAIN_NODATA","","NOT_APPLY","","","","Non
e","","","DESCENDING","BLEND","13","","","","","","FULL","","DISABLED","","","
","","","","")

arcpy.BuildSeamlines_management(Mosiac2, "","NORTH_WEST", "#", "#", "#",
"#","RADIOMETRY", "10", "BOTH", "#", "#")
#Make Mosiac a Tiff
arcpy.CopyRaster_management(Mosiac2, str(final_newpath) + "/" + "final")
print "finished!"
```